

Weather Research and Forecasting Model Sensitivity Comparisons for Warm Season Convective Initiation

Leela R. Watson
*Applied Meteorology Unit
Kennedy Space Center, Florida*

August 2007

NASA STI Program ... in Profile

Since its founding, NASA has been dedicated to the advancement of aeronautics and space science. The NASA scientific and technical information (STI) program plays a key part in helping NASA maintain this important role.

The NASA STI program operates under the auspices of the Agency Chief Information Officer. It collects, organizes, provides for archiving, and disseminates NASA's STI. The NASA STI program provides access to the NASA Aeronautics and Space Database and its public interface, the NASA Technical Report Server, thus providing one of the largest collections of aeronautical and space science STI in the world. Results are published in both non-NASA channels and by NASA in the NASA STI Report Series, which includes the following report types:

- **TECHNICAL PUBLICATION.** Reports of completed research or a major significant phase of research that present the results of NASA Programs and include extensive data or theoretical analysis. Includes compilations of significant scientific and technical data and information deemed to be of continuing reference value. NASA counterpart of peer-reviewed formal professional papers but has less stringent limitations on manuscript length and extent of graphic presentations.
- **TECHNICAL MEMORANDUM.** Scientific and technical findings that are preliminary or of specialized interest, e.g., quick release reports, working papers, and bibliographies that contain minimal annotation. Does not contain extensive analysis.
- **CONTRACTOR REPORT.** Scientific and technical findings by NASA-sponsored contractors and grantees.

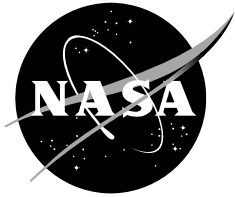
- **CONFERENCE PUBLICATION.** Collected papers from scientific and technical conferences, symposia, seminars, or other meetings sponsored or co-sponsored by NASA.
- **SPECIAL PUBLICATION.** Scientific, technical, or historical information from NASA programs, projects, and missions, often concerned with subjects having substantial public interest.
- **TECHNICAL TRANSLATION.** English-language translations of foreign scientific and technical material pertinent to NASA's mission.

Specialized services also include creating custom thesauri, building customized databases, and organizing and publishing research results.

For more information about the NASA STI program, see the following:

- Access the NASA STI program home page at <http://www.sti.nasa.gov>
- E-mail your question via the Internet to help@sti.nasa.gov
- Fax your question to the NASA STI Help Desk at (301) 621-0134
- Phone the NASA STI Help Desk at (301) 621-0390
- Write to:
NASA STI Help Desk
NASA Center for AeroSpace Information
7121 Standard Drive
Hanover, MD 21076-1320
-

NASA/CR—2007–214734



Weather Research and Forecasting Model Sensitivity Comparisons for Warm Season Convective Initiation

Leela R. Watson
*Applied Meteorology Unit
Kennedy Space Center, Florida*

August 2007

Acknowledgments

The author thanks Mr. Brian Hoeth of the Spaceflight Meteorology Group, Mr. Pete Blottman and Mr. David Sharp of the National Weather Service in Melbourne, FL, and Mr. William Roeder of the 45 Weather Squadron for their valuable feedback and suggestions and Dr. Francis J. Merceret of the Kennedy Space Center Weather Office for his review and suggestions.

Available from:

NASA Center for AeroSpace Information
7121 Standard Drive
Hanover, MD 21076-1320
(301) 621-0390

This report is also available in electronic form at

<http://science.ksc.nasa.gov/amu/>

Executive Summary

Mesoscale weather conditions can have an adverse affect on space launch, landing, ground processing, and weather advisories, watches, and warnings at Kennedy Space Center (KSC) and Cape Canaveral Air Force Station (CCAFS). During the summer months, land-sea interactions that occur across KSC and CCAFS lead to the formation of a sea breeze, which can spawn deep convection. These convective processes often last 60 minutes or less and pose a significant challenge to the forecasters at the National Weather Service (NWS) Spaceflight Meteorology Group (SMG), NWS Melbourne, Florida (MLB), and the 45th Weather Squadron (45 WS). As a result of this challenge, the need for accurate mesoscale model forecasts to aid in their decision making is crucial.

The current state-of-the-art mesoscale Weather Research and Forecasting (WRF) model provides the user with many different model configuration options. It has two dynamical cores – the Advanced Research WRF (ARW) and the Non-hydrostatic Mesoscale Model (NMM). In addition to the two dynamical cores, there are also two data analysis packages that can provide initialization data for the model – the Local Analysis and Prediction System (LAPS) and the Advanced Regional Prediction System (ARPS) Data Analysis System (ADAS). Besides model core and initialization options, the WRF model can be run with one- or two-way nesting. Having a series of initialization options and WRF cores, as well as many options within each core, provides SMG and MLB with considerable flexibility as well as decision-making challenges. The Applied Meteorology Unit (AMU) was tasked to compare the WRF model performance using ADAS versus LAPS for the ARW and NMM model cores and to compare the impact of using a high-resolution local forecast grid with one-way, two-way, and no nesting, as well as to examine the impact of assimilating soil moisture data on model performance.

Five convective initiation days and two null, non-convection days were chosen to assess model skill. To compare the three different combinations of WRF initializations, ADAS-ARW, LAPS-ARW, and LAPS-NMM, the WRF model was run at a 4 km horizontal grid spacing over the Florida peninsula and adjacent coastal waters. Each run was integrated 12 hours with three runs per day initialized at 0900, 1200, and 1500 UTC. Boundary conditions were obtained from the North American Mesoscale (NAM) model, while initial conditions were obtained from the Rapid Update Cycle (RUC) model. Data ingested by the model through either the LAPS or ADAS analysis packages included Level II Weather Surveillance Radar-1988 Doppler (WSR-88D) data, Geostationary Operational Environmental Satellites (GOES) visible and infrared satellite imagery, and surface observations throughout Florida. To compare the performance of the WRF model using a high-resolution local grid with one-way, two-way, and no nesting, the inner nest was run with a grid spacing of 1.33 km over east-central Florida.

To verify precipitation, forecast rainfall accumulation was compared to the NCEP stage-IV analysis. To determine the skill of each model configuration, the Fractions Skill Score (FSS), an objective precipitation verification method, was employed. This method calculates a probability of precipitation for each grid square based on the assumption that the model is in error on the scale of the size of the area used to produce the fractions. In addition to an objective precipitation verification method, a subjective verification was also performed for select convective initiation cases.

Some of the key results found include the following:

- All model configurations suffered from model spin up of too much precipitation in area and amount.
- Beyond six hours, all model configurations increased in skill.
- The difference in skill between the ADAS-ARW and LAPS-ARW was negligible, while the skill of LAPS-NMM was slightly worse.
- The use of a local high-resolution grid did not significantly improve the skill of the model as compared to the coarser model runs.
- The analysis of all hot-start model configurations and nesting configurations indicated that no single model was clearly better than the rest.

These results suggest that high-resolution forecasts over Florida during the warm season are best to help develop a broad understanding of a situation rather than in predicting individual convective cells.

Table of Contents

Executive Summary.....	3
Table of Contents.....	4
List of Figures.....	5
List of Tables.....	7
1. Introduction.....	8
1.1 Background Information.....	8
1.2 Model Configuration Options.....	9
1.3 Report Format and Outline.....	9
2. Data and Methodology.....	10
2.1 Choosing Candidate Days.....	10
2.2 Model Core and Initialization Options.....	10
2.3 Nesting Options.....	12
2.4 Soil Moisture Assimilation.....	13
2.5 Precipitation Verification.....	14
3. Comparison of WRF Model Initializations.....	16
3.1 Forecast Bias.....	16
3.2 Fractions Skill Score in Space.....	16
3.3 Fractions Skill Score in Space and Time.....	20
3.4 Subjective Evaluation.....	21
4. Comparison of Nesting Options.....	26
4.1 Forecast Bias.....	26
4.2 Fractions Skill Score in Space.....	26
4.3 Fractions Skill Score in Space and Time.....	26
4.4 Subjective Evaluation.....	30
5. Soil Moisture Assimilation.....	33
6. Conclusions.....	34
6.1 Results.....	34
6.2 Recommendations.....	35
6.3 Possible Future Work.....	35
References.....	36
List of Acronyms.....	40
NOTICE.....	41

List of Figures

Figure 1.	The distribution of a) WSR-88D data and b) surface observations over the Florida peninsula.....	12
Figure 2.	The WRF domains for the 4 km (outer box) and 1.33 km grids (inner box).....	13
Figure 3.	A schematic to show how fractions are computed for the FSS equation. See text for explanation.	15
Figure 4.	The forecast bias of rainfall accumulation (mm) versus time (UTC) for ADAS-ARW (top), LAPS-ARW (middle), and LAPS-NMM (bottom). The black line is the hourly observed rainfall accumulation averaged over the 4 km domain. The red, green, and blue lines are the averaged forecast rainfall accumulations for all model runs initialized at 0900, 1200, and 1500 UTC, respectively.....	17
Figure 5.	The Fractions Skill Score versus forecast hour for ADAS-ARW (top), LAPS-ARW (middle), and LAPS-NMM (bottom). The colored lines represent model skill on different spatial scales, from the grid scale at 4 km to 160 km. The color legend is on the bottom of each chart.	18
Figure 6.	The range of spatial scales for the FSS calculations, starting from the grid scale at 4 km (center point) to 160 km. The center point of each circle is located at LC 39A.	19
Figure 7.	Change in skill when one- and two-hour temporal scales were taken into account for all three WRF model configurations over the range of spatial scales shown in Figure 6. The legend showing the color of each curve for each model and temporal scale combination is in the upper right.	20
Figure 8.	The a) observed composite reflectivity valid at 1500 UTC 17 July 2006 and b) ADAS-ARW, c) LAPS-ARW, and d) LAPS-NMM three-hour forecasts of composite reflectivity initialized at 1200 UTC 17 July 2006.....	21
Figure 9.	The a) observed composite reflectivity valid at 1800 UTC 17 July 2006 and b) ADAS-ARW, c) LAPS-ARW, and d) LAPS-NMM six-hour forecasts of composite reflectivity initialized at 1200 UTC 17 July 2006.....	22
Figure 10.	The a) observed composite reflectivity valid at 2100 UTC 17 July 2006 and b) ADAS-ARW, c) LAPS-ARW, and d) LAPS-NMM nine-hour forecasts of composite reflectivity initialized at 1200 UTC 17 July 2006.....	23
Figure 11.	The a) observed composite reflectivity valid at 0000 UTC 18 July 2006 and b) ADAS-ARW, c) LAPS-ARW, and d) LAPS-NMM 12-hour forecasts of composite reflectivity initialized at 1200 UTC 17 July 2006.....	24
Figure 12.	The forecast bias of rainfall accumulation (mm) versus time (UTC) for LAPS-ARW 1.33 km nest using one-way (top), two-way (middle), and no nesting (bottom). The black line is the hourly observed rainfall accumulation averaged over the 1.33 km domain. The red, green, and blue lines are the averaged forecast rainfall accumulations for all model runs initialized at 0900, 1200, and 1500 UTC, respectively.	27
Figure 13.	The Fractions Skill Score versus forecast hour for LAPS-ARW 1.33 km nest using one-way (top), 2-way (middle), and no nesting (bottom). The colored lines represent model skill on different spatial domains, from the grid scale of 1.33 km to 53.2 km. The color legend is on the bottom of each chart.	28
Figure 14.	Range of spatial scales FSS was computed over for the 1.33 km nested runs. Circle A represents 5.3 km, B represents 13.3 km, C represents 26.6 km, D represents 53.2 km. The center point of each circle, which represents the grid scale, is located at LC 39A.	29
Figure 15.	Change in skill when one- and two-hour temporal scales were taken into account for all three LAPS-ARW nesting configurations over the range of spatial scales shown in Figure 14. The legend showing the color of each curve for each model and temporal scale combination is in the lower right.	29

Figure 16. The a) observed composite reflectivity valid at 1500 UTC 17 July 2006 and b) 1-way, c) 2-way, and d) no nesting three-hour forecasts of composite reflectivity initialized at 1200 UTC 17 July 2006	30
Figure 17. The a) observed composite reflectivity valid at 1800 UTC 17 July 2006 and b) 1-way, c) 2-way, and d) no nesting six-hour forecasts of composite reflectivity initialized at 1200 UTC 17 July 2006	31
Figure 18. The a) observed composite reflectivity valid at 2100 UTC 17 July 2006 and b) 1-way, c) 2-way, and d) no nesting nine-hour forecasts of composite reflectivity initialized at 1200 UTC 17 July 2006	31
Figure 19. The a) observed composite reflectivity valid at 0000 UTC 18 July 2006 and b) 1-way, c) 2-way, and d) no nesting 12-hour forecasts of composite reflectivity initialized at 1200 UTC 17 July 2006	32

List of Tables

Table 1. List of the convection and non-convection days used in the study and the corresponding average surface wind speed and direction at 1200 UTC at Melbourne, FL for each candidate day.10

Table 2. List of the physics options used for each model run for both the ARW and NMM cores.....11

1. Introduction

Mesoscale weather conditions can have an adverse affect on space launch, landing, ground processing, and weather advisories, watches, and warnings at Kennedy Space Center (KSC) and Cape Canaveral Air Force Station (CCAFS). During summer, land-sea interactions across KSC and CCAFS lead to sea breeze formation, which can spawn deep convection. These convective processes often last 60 minutes or less and pose a significant challenge to the forecasters at the National Weather Service (NWS) Spaceflight Meteorology Group (SMG). The main challenge is that a “GO” or “No GO” forecast for thunderstorms at the Shuttle Landing Facility is required at the 90 minute deorbit decision for End Of Mission and at the 30 minute Return To Launch Site decision after launch. Convective initiation, timing, and mode also present a forecast challenge for the NWS in Melbourne, FL (MLB). The NWS MLB issues such forecast information as Terminal Aerodrome Forecasts, Spot Forecasts for fire weather and hazardous materials incident support, and severe/hazardous weather Watches, Warnings, and Advisories. These forecasting challenges can also affect the 45th Weather Squadron (45 WS), which provides weather forecasts for space launches, ground operations, and weather advisories, watches, and warnings for personnel safety and resource protection at KSC and CCAFS. Accurate mesoscale model forecasts to aid in their decision making are needed.

As a result of these challenges, the Applied Meteorology Unit (AMU) was tasked to determine the skill of different Weather Research and Forecasting (WRF) model configurations in forecasting warm season convective initiation. The WRF model has two dynamical cores: 1) the Advanced Research WRF (ARW) and 2) the Non-hydrostatic Mesoscale Model (NMM). There are also two options for a “hot-start” initialization of the WRF model: 1) the Local Analysis and Prediction System (LAPS; McGinley 1995) and 2) the Advanced Regional Prediction System (ARPS) Data Analysis System (ADAS; Brewster 1996). Both LAPS and ADAS are three-dimensional weather analysis systems that integrate multiple meteorological data sources into one analysis over the user’s domain of interest. These analysis systems allow mesoscale models to benefit from the addition of high-resolution data sources in their initial conditions. In addition to model core and initialization options, the WRF model can be run with one- or two-way nesting. Nesting allows a high-resolution forecast grid to be run within a coarser domain. Having a series of initialization options and WRF cores, as well as many options within each core, provides SMG and MLB with considerable flexibility as well as decision-making challenges. The goal of this study is to assess the different model configurations and to determine which configuration will best predict warm season convective initiation. To accomplish this, the AMU compared the WRF model performance using ADAS versus LAPS for the ARW and NMM cores, compared the impact of using a high-resolution local forecast grid with two-way, one-way, and no nesting, and examined the impact of assimilating local soil moisture sensor data on WRF performance.

1.1 Background Information

Numerous factors influence the development of convection over the Florida peninsula. During the summer, synoptic scale forcing over Florida is weak and most convection is forced by the mesoscale (Lericos et al. 2002). Such mesoscale processes include sea breezes, river and lake breezes, convergent flow due to convex coastlines that enhance sea breeze convergence over land (Laird et al. 1995; Lericos et al. 2002; McPherson 1970; Pielke 1974), shear lines from washed out fronts, weak upper-air short waves, weak speed streaks, cloud shadow breezes, and even soil moisture gradients. The interaction of these processes produces the warm season convective patterns seen over the Florida peninsula (Manobianco and Nutter 1998). In addition, regeneration of convection can occur due to the collision of outflow boundaries (Fovell 2005; Simpson et al. 1980; Tao and Simpson 1984; Purdom 1982; Droegemeier and Wilhelmson 1985). However, warm season convection remains one of the most poorly forecast meteorological parameters, in part due to dynamic and thermodynamic features that occur on the mesoscale (Jankov et al. 2005; Fowle and Roebber 2003).

Previous numerical modeling studies of warm season convection identified some factors that can affect the skill of the model. Many of the studies focused on the difference in skill among different convective parameterization schemes. Since the model used in this study was run with explicit convection, a review of those studies that focus solely on convective parameterization is not presented here. In a study by Lynn et al. (2001), model performance improved due to three elements: the initial soil moisture and temperature, the use of a land surface model, and an improved turbulence parameterization. The initial soil moisture and temperature fields were essential for determining the surface temperature perturbations, while the land surface model was essential for modifying these fields. They found that a land surface model and an improved turbulence parameterization showed the most benefit for predicting warm season, weakly forced convection. Fowle and Roebber (2003) concluded that forecasts of

precipitation were also sensitive to the uncertainty in atmospheric initial conditions, whose differences can lead to widely different precipitation forecasts. The importance of a comprehensive and accurate analysis of the state of the atmosphere for the forecast initial conditions is vital to improving model skill. Another study conducted by Jankov et al. (2005) found that the choice of a microphysical scheme impacted the total rain volume of warm season convection. Gallus and Bresch (2006) extended these results and found that total rain volume was more sensitive to the choice of dynamical core rather than the chosen microphysical scheme, while the opposite was true for the model peak rain rate. In addition, they found that the intensity and location of rainfall was influenced by the chosen dynamical core.

1.2 Model Configuration Options

As stated earlier, the WRF numerical weather modeling system consists of two dynamical cores, ARW and NMM. The ARW core was developed primarily at the National Center for Atmospheric Research (NCAR) while the NMM was developed at the National Centers for Environmental Prediction (NCEP). The work described in this report employed the WRF Environmental Modeling System (EMS) software, which was developed by the NWS Science Operations Officer (SOO) Science and Training Resource Center (STRC). A benefit of using the WRF EMS is that it incorporates both dynamical cores into a single end-to-end forecasting model (Rozumalski 2006). The software consists of pre-compiled programs that are easy to install and run. The WRF EMS contains the full physics options available for the ARW and NMM cores, however, the physics options for the NMM are more limited than for the ARW. The software also supports two- and one-way nesting.

The two local data analysis systems mentioned earlier, LAPS and ADAS, were used to hot-start the WRF model. Hot-start initialization improves the short term forecast by including all microphysics, such as rain, snow, and cloud water, in the forecast initial conditions while ensuring the model is in dynamic balance with the mass and momentum fields (Schultz and Albers 2001; McGinley and Smart 2001; Shaw et al. 2001).

1.3 Report Format and Outline

This report presents the findings from a one year study of model sensitivities for predicting warm season convective initiation over Florida. This analysis examined different model initializations, nesting configurations, and explored the use of soil moisture data in the model initial conditions to determine the impact on model skill. Two local data analysis systems that ingested satellite data, radar data, and surface observations across the Florida peninsula were used to initialize a mesoscale model. Model skill was assessed using an objective verification technique that compared forecast rainfall accumulation to a one-hourly precipitation analysis available from NCEP. Section 2 describes the data and methodology including the different model cores, model initialization options, nesting options, soil moisture assimilation, and the method used to verify precipitation. The results of the model initialization and nesting comparisons are presented in Sections 3 and 4, respectively. Section 5 describes some techniques for assimilating soil moisture into a mesoscale model. Section 6 summarizes the report and provides recommendations on the best mesoscale model configuration for operational use based on this study.

2. Data and Methodology

The important aspects of this study were the choice of candidate convective initiation days, the model configurations, the data used to initialize the models, and the choice of an objective precipitation verification method. Candidate convective initiation days were chosen over the Jun – Sep 2006 season. Comparisons were made between the ARW and NMM core initialized with ADAS and LAPS, as well as different nesting configurations. To verify precipitation, the objective precipitation verification method called Fractions Skill Score (FSS) (Roberts 2005) was employed.

2.1 Choosing Candidate Days

Candidate convective initiation days were chosen based on the timing of the onset of convection, the amount of convection over the peninsula during each forecast period and in particular over the KSC/CCAFS area, and the availability of data. Since the goal of this study was to assess model skill in forecasting convective initiation, WRF simulations that had numerous active convective cells in the initial conditions were not considered for evaluation. This limited potential days to those in which convection began between 1600 and 2100 UTC. Potential days were also evaluated for the amount of convection occurring across Florida. Days that did not exhibit numerous storms over the forecast period were not considered. Days consisting of dominant synoptic-scale forcing patterns were not considered. Candidate days were chosen as follows. First, days with missing data were identified. Twenty days were missing data from Jun – Sep 2006. Next, time of convection onset and presence of synoptic scale forcing were accounted for. Of the days with available data, 34 were determined to be potential convective initiation days. Third, a subjective evaluation was made to determine if a significant amount of convection occurred throughout the forecast period. If the candidate day did not exhibit numerous convective cells across the peninsula with a minimum composite reflectivity threshold of 20 dBZ between 1600 and 0000 UTC, it was rejected. This limited the candidate days to approximately 20. However, based on the amount of time allocated to the task, only a handful of days could be chosen. Of the 20 potential days, the five best convective initiation days were chosen (Table 1). Two null, or non-convection, days were also chosen. It is important to note that it was virtually impossible to find days during the summer season with no rain over the Florida peninsula. Therefore, days that had minimal rain were chosen for the null days. The results presented in this report are limited by the number of candidate days. While a study of the full convective season would be ideal, it was felt that using a handful of representative days would help in obtaining an overall view of the skill of each model configuration.

Table 1. List of the convection and non-convection days used in the study and the corresponding average surface wind speed and direction at 1200 UTC at Melbourne, FL for each candidate day.

		Wind Speed (mph)	Wind Direction
Convection Days	5 July 2006	7.6	East
	7 July 2006	6.6	Southeast
	17 July 2006	4.7	South-Southeast
	17 August 2006	4.2	East-Southeast
	2 September 2006	8.1	South-Southeast
Non-convection Days	1 July 2006	8.8	East-Northeast
	4 July 2006	10.0	East-Northeast

2.2 Model Core and Initialization Options

The first part of the task compared three different combinations of WRF initializations, ADAS-ARW, LAPS-ARW, and LAPS-NMM, to determine their skill at forecasting warm season convection. A hot-start initialization of the NMM model using ADAS could not be completed as the WRF EMS software does not support this configuration. The code continually sets the microphysics to 0, precluding the hot-start initialization option. The ARW core is a fully compressible, non-hydrostatic mesoscale model with a hydrostatic option. It consists of a mass-based hydrostatic pressure terrain following coordinate, Arakawa C-grid staggering for the horizontal grid, time-split integration using a third order Runge-Kutta scheme with a small step for acoustic and gravity wave modes, and up to sixth order advection options in the horizontal and vertical (Skamarock et al. 2005). There are also full physics

options for microphysics, planetary boundary layer, cumulus parameterization, radiation, and land surface schemes (Skamarock et al. 2005). The ARW core includes the option of running two- and one-way nests. In both nesting types, the coarse grid supplies the boundary conditions for the fine grid. In a one-way nest, the information exchange is from the coarse grid to the fine grid only, whereas in a two-way nest, information is exchanged from the coarse grid to the fine grid and vice versa (Skamarock et al. 2005). The NMM core is also a fully compressible, non-hydrostatic mesoscale model with a hydrostatic option (Janjic et al. 2001, Janjic 2003a,b). It consists of a hybrid sigma-pressure, terrain following vertical coordinate, Arakawa E-grid, a forward-backward time integration scheme, a second order advection option in the horizontal and vertical, and conservation of energy and enstrophy (Janjic 1984). Most physics packages available to the ARW have not been tested with the NMM and therefore, the physics options for the NMM are more limited than for the ARW.

Each model simulation was run at a 4 km horizontal grid spacing over the Florida peninsula and adjacent coastal waters with 40 irregularly spaced, vertical sigma levels. Each run was integrated 12 hours with three runs per day for the seven case days, at 0900, 1200, and 1500 UTC, for a total of 21 model runs. Table 2 lists the physics options used in both the ARW and NMM runs. It should be noted that 4 km grid spacing is inadequate to capture some important boundary interactions for Florida summer convection, such as the Indian River and Banana River breezes in the KSC/CCAFA area. A grid spacing of ≤ 1 km is needed to detect and resolve these local river breezes.

Table 2. List of the physics options used for each model run for both the ARW and NMM cores.		
	ARW	NMM
Microphysical scheme	Lin et al. (1983)	Lin et al. (1983)
Planetary boundary layer scheme	Mellor-Yamada-Janjic (Janjic 1990, 1996, 2002)	Mellor-Yamada-Janjic (Janjic 1990, 1996, 2002)
Land surface option	Noah Land Surface Model (Chen and Dudhia 2001)	Noah Land Surface Model (Chen and Dudhia 2001)
Surface layer scheme	Janjic Eta (Janjic 1996, 2002)	Janjic Eta (Janjic 1996, 2002)
Shortwave radiation scheme	Goddard (Chou and Suarez 1994)	GFDL (Lacis and Hansen 1974)
Longwave radiation scheme	RRTM (Mlawer et al. 1997)	GFDL (Fels and Schwarzkopf 1975; Schwarzkopf and Fels 1985, 1991)

Boundary conditions were obtained from NCEP's North American Mesoscale (NAM) model with a horizontal grid spacing of 40 km, while initial conditions were obtained from the NCEP's Rapid Update Cycle (RUC) model also with a horizontal grid spacing of 40 km. The RUC was designed to provide numerical forecast guidance for a 12-hour period (Benjamin et al. 1998). It assimilates observations every hour at the surface and aloft and is run every three hours, or eight times per day, which is the highest frequency of all forecast models at NCEP. The RUC domain is on a Lambert conformal projection with a horizontal domain size of 151 by 113 grid points and includes 40 vertical levels. The NAM domain is also on a Lambert conformal projection with a horizontal domain size of 185 by 129 grid points and 39 vertical levels. The NAM model produces an 84-hour forecast every six hours, or four times per day. The NAM model was chosen for boundary conditions to allow for longer WRF forecasts.

The LAPS system is a data assimilation tool that uses numerous meteorological observations, such as satellite data, radar data, and surface observations, to generate a three-dimensional representation of the atmospheric forcing fields, such as wind speed and direction, surface temperature and pressure, relative humidity, precipitation and cloud cover (McGinley et al. 1991; Albers 1995; Albers et al. 1996; Birkenheuer 1999; McGinley 1995). The LAPS system includes a wind analysis and a three-dimensional cloud analysis, which is needed for the LAPS hot-start initialization. The LAPS cloud analysis is designed to create consistency with all data and the typical meteorology of clouds by combining data from infrared and visible satellite data, three-dimensional LAPS radar reflectivity derived from the full volume radar data, and the LAPS three-dimensional temperatures (Albers et al. 1996). Fields derived from the cloud analysis include cloud liquid water, cloud type, cloud droplet size, and icing severity (Albers et al. 1996). The ADAS (Brewster 1996), developed by the University of Oklahoma, has two main components. The first is a Bratseth objective analysis scheme that evaluates pressure, wind, potential temperature, and specific humidity. The second component is a three-dimensional cloud analysis scheme that is used for the hot-start initialization (Zhang et al. 1998). The ADAS cloud analysis is based on the LAPS cloud analysis with some modifications (Case et al. 2002). It uses surface observations of cloud cover and height, satellite data, and radar data to determine the

cloud cover, cloud liquid and ice water, cloud type, rain/snow/hail mixing ratios, icing severity, in-cloud vertical velocity, cloud base and top, and cloud ceiling (Case et al. 2002; Zhang et al. 1998; Brewster 2002).

Data ingested by the model through either the LAPS or ADAS analysis packages included Level II Weather Surveillance Radar-1988 Doppler (WSR-88D) data from all Florida radars (Figure 1a), Geostationary Operational Environmental Satellites (GOES) visible and infrared satellite imagery, and surface observations throughout Florida (Figure 1b). The Level II WSR-88D data contained full volume scans of reflectivity at a resolution of 1 degree by 1 km, radial velocity at a 1 degree by 0.25 km, and spectrum width data at a 1 degree by 0.25 km (Fulton et al. 1998). These data were available every 4 to 6 minutes. The GOES-12 visible imagery was available at a 1 km horizontal resolution every 15 minutes, and the infrared imagery was available at a 4 km horizontal resolution also every 15 minutes. Both visible and infrared imagery provided brightness temperatures to the analysis packages. Surface observations from the Florida Automated Weather Network (FAWN) and from buoy/ship reports were available throughout Florida, and are represented in Figure 1b. Measured variables include u- and v-wind components, temperature, dewpoint temperature, pressure, and sea surface temperature. These data were available at a combined horizontal resolution of 34 km (Case 1999).

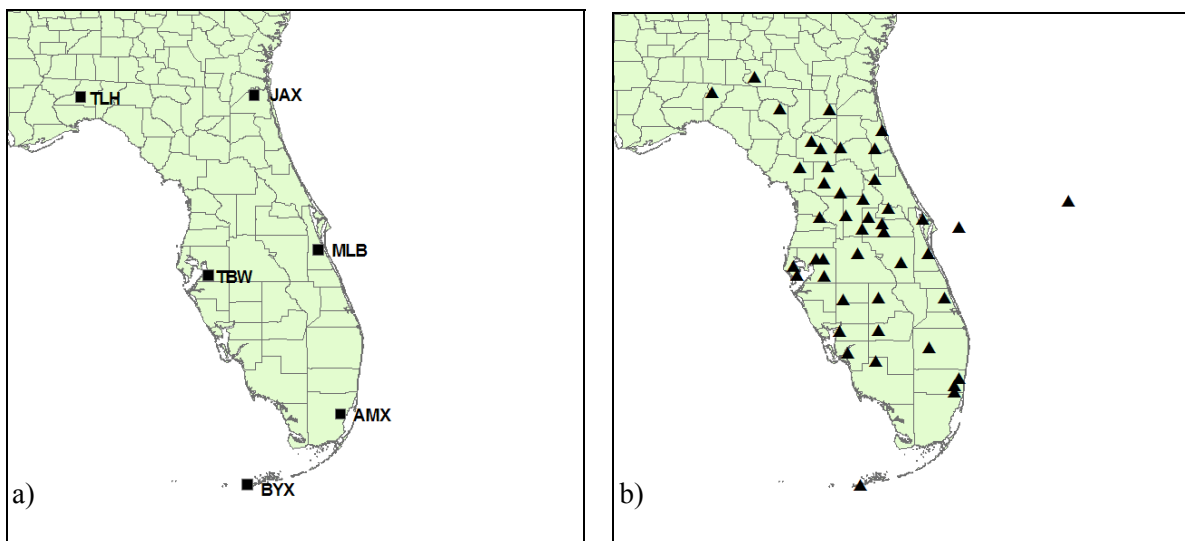


Figure 1. The distribution of a) WSR-88D data and b) surface observations over the Florida peninsula.

A suite of scripts written by the AMU formed the core for initializing the WRF model with ADAS output. The WRF EMS was run as if in real-time, ingesting satellite data in Man computer Interactive Data Access System (McIDAS) Area format 15 minutes prior to model initialization time; raw, full volume, radar data within 10 minutes of the model initialization time; and surface data from the hour of and hour prior to model initialization. The largest task in configuring LAPS was working with the ingest code. The ingest code can only be used with raw data that have the same configuration and format as the National Oceanic and Atmospheric Administration Earth System Research Laboratory Global Systems Division's (GSD) raw data, which is the Network Common Data Form (NetCDF). Therefore, all data files were converted to NetCDF format to be used within LAPS. Software to convert the WSR-88D data and model data to NetCDF format was obtained from GSD. A FORTRAN program was written by the AMU to reformat the surface data to a form usable by LAPS. Converting satellite data in McIDAS Area format to NetCDF required several steps. The data were first ported to the local Meteorological Interactive Data Display System (MIDDS) system where they were remapped to the Lambert Conformal projection using the IMGREMAP command. Next, the remapped data were run through a program that converted them to NetCDF format. This program is called AreaToNetCDF and is available from the Space Science and Engineering Center (SSEC) at the University of Wisconsin. All of the reformatted data files were then ingested into LAPS to create an initialization field for the model.

2.3 Nesting Options

The second part of this task included a comparison of the performance of LAPS-ARW using a high-resolution local grid with two-way, one-way, and no nesting for all convective initiation cases. In two-way nesting the outer,

coarse domain provides the boundary conditions to the inner fine-mesh grid, and the inner grid feeds back the higher resolution forecast to the outer grid (Gill et al. 2004). The fine-mesh domain is initialized by the interpolation of the coarse, outer domain. One-way nesting is the same as two-way nesting except that the inner grid does not feed back to the outer grid.

For this task, as shown in Figure 2, the nested fine-mesh inner grid covered the east-central Florida region and the coarse-mesh outer grid included all of peninsular Florida and adjacent coastal waters. The inner grid had a grid spacing of 1.33 km, while the outer grid had a grid spacing of 4 km. Both grids had 40 irregularly spaced, vertical sigma levels. Due to limitations in the NMM core, only the ARW core could be used for nested model runs. The LAPS-ARW configuration was chosen based on a comparison of results from the 4 km ADAS-ARW and LAPS-ARW model runs. Although the objective analysis for both models was similar, a subjective verification suggested the LAPS-ARW configuration slightly outperformed the ADAS-ARW in the early hours of the forecast.

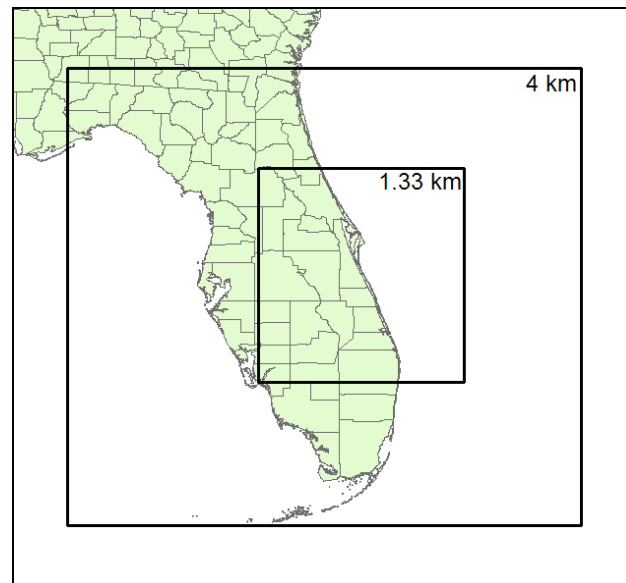


Figure 2. The WRF domains for the 4 km (outer box) and 1.33 km grids (inner box).

2.4 Soil Moisture Assimilation

The third part of this task was examining the impact of assimilating KSC soil moisture sensor data on WRF model performance. Soil moisture data can be crucial to forecasting land surface exchange processes (Pleim and Xiu 2003). These land surface exchange processes affect the structure of the planetary boundary layer and the associated clouds and precipitation (Xiu and Pleim 2001). In particular, soil moisture can affect surface latent heat fluxes (Chen and Dudhia 2001). Chen and Dudhia (2001) found that forecast surface heat flux from a coupled Pennsylvania State University/NCAR mesoscale model (MM5)-land surface model (LSM) was sensitive to the initial soil moisture field. For dry soils, a change of 10% in the initial soil moisture caused a 30 W m^{-2} variation in surface heat fluxes, while a change of 0.1 in initial soil moisture in terms of its volumetric value caused a change of 200 W m^{-2} . An increase in surface latent heat flux leads to an increase in the evaporation of water, leading to increased clouds and precipitation. For moist soils, the effect was similar.

Currently, ADAS cannot assimilate and analyze in situ soil moisture data into its analysis. Therefore, in the original task it was determined that sensitivity tests involving soil moisture would have to be conducted using LAPS. After further research, it became apparent that LAPS was also unable to assimilate soil moisture data for the following reasons: (1) The LAPS soil moisture algorithm provides a three-layer analysis of soil moisture (0 to 6 in, 6 to 12 in, and 12 to 36 in) and does not provide a soil temperature analysis. The WRF EMS software requires input of soil moisture and soil temperature data on at least four levels. This code was written such that if less than four layers of soil data were available from LAPS, none of the LAPS soil data were used in the analysis. Rather, all soil moisture and temperature data would come from a specified land surface data set; (2) Soil moisture data at KSC is

available at a depth of 1.2 in (3 cm), integrated over a depth of 1.2 to 3.9 in (3 to 10 cm), and integrated over 15 to 29.9 in (38 to 76 cm) below the surface. Even if the LAPS soil analysis could be used with the WRF EMS, LAPS only ingests one level of soil moisture data, but the level needed is not specified anywhere in the code; (3) Lastly, LAPS does not currently utilize any soil moisture data within the soil moisture algorithm, nor does it use the soil moisture data for deriving any other atmospheric variable. Therefore, alternative methods that can be used to ingest soil moisture data into the WRF model are explored in Section 5.

2.5 Precipitation Verification

To verify precipitation, hourly forecast rainfall accumulation was compared to the NCEP stage-IV analysis (Fulton et al. 1998). This analysis combines radar data and rain gauge reports to produce hourly rainfall accumulation on a 4 km grid. It is a manually quality-controlled CONUS mosaic from the regional 1-hr precipitation analyses produced by 12 NWS River Forecast Centers (RFCs) (Lin and Mitchell 2005).

To determine the skill of each model configuration, the FSS (Roberts 2005) was employed. The FSS is an objective precipitation verification method based on the Brier Skill Score that answers the question of what spatial scales the forecast resembles the observations. The method involves computing a fraction for each grid square based on the number of surrounding grid squares in which precipitation occurred. This gives a fraction, or a probability of precipitation, for each grid square based on the assumption that the model is in error on the scale of the size of the area used to produce the fractions. By changing the size of the area, fractions can be produced for different spatial scales. Figure 3 gives an example of how fractions are computed over different sized squares. The red squares indicate areas where precipitation has occurred, while the white squares indicate no precipitation. For this example, fractions are computed for the grid square marked with an X using two different spatial scales, squares A and B. Using a grid square length of 4 km, square A is 12 x 12 km and square B is 28 x 28 km. The fraction at the grid square X computed over square A (3 by 3 squares) is 2/9, or 0.22. This indicates that the probability of precipitation within 12 km of the grid square marked with an X is 22%. The fraction at the grid square X computed over square B (7 by 7 squares) is 13/28, or 0.46. Fractions are computed in the same way for both the model and observed rainfall accumulations so that they can be compared. For this study, fractions were computed using 1, 5, 10, 20, and 40 grid squares such that the range of spatial scales for the 4 km runs ranged from 4 to 160 km, while the range of spatial scales for the 1.33 km runs ranged from 1.33 to 53.2 km. Once the fractions are obtained, FSS is computed as:

$$FSS = 1 - \frac{FBS}{\frac{1}{N} \left[\sum_{j=1}^N (p_j)^2 + (o_j)^2 \right]},$$

where FBS is the Fractions Brier Score computed as:

$$FBS = \frac{1}{N} \sum_{j=1}^N (p_j - o_j)^2,$$

where p_j is the forecast fraction, o_j is the observed fraction, and N is the total number of grid box fractions. The values of FSS range from 0 to 1, in which 1 indicates a perfect forecast and 0 indicates no skill. It is intuitive that as the spatial scale of the fractions increases, so should the skill. However, the FSS will asymptote at some value determined by the forecast bias. The smaller forecast bias, the closer the asymptotic value is to 1. The FSS is most sensitive to small rain events and is least skillful at the forecast grid scale.

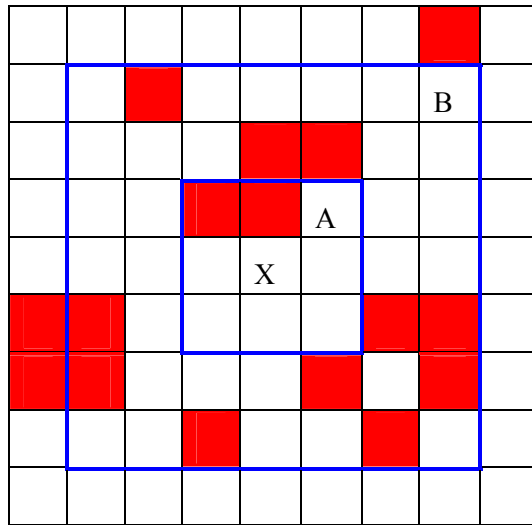


Figure 3. A schematic to show how fractions are computed for the FSS equation. See text for explanation.

In addition to an objective precipitation verification method, a subjective verification was also performed for select convective initiation cases. Although FSS can illustrate the spatial and temporal skill of the model and can be used to compare model performance, it does not provide information on why a forecast was good or bad. To remedy this, a subjective evaluation was used to compare the forecast composite reflectivity to the observed composite reflectivity. One of those cases is shown in Sections 3.4 and 4.4.

3. Comparison of WRF Model Initializations

A comparison of hourly model rainfall accumulation to stage-IV rainfall accumulation analyses was made for each forecast for all convection and non-convection days. The stage-IV data was averaged to the same grid as the mesoscale model to give a similar comparison. In addition to assessing the spatial and temporal accuracy of the different model configurations, it was important to assess the accuracy of the predicted amounts of rainfall in the verification area, or the forecast bias. It is important to note that the results presented here are limited in scope due to the number of candidate convective initiation days chosen.

3.1 Forecast Bias

Figure 4 shows the forecast bias for the ADAS-ARW, LAPS-ARW, and LAPS-NMM model configurations, respectively. It is apparent that both ADAS-ARW and LAPS-ARW over-predicted rainfall significantly during the first five to six hours of each forecast. Both configurations also showed sharp increases in rainfall accumulation within the first two hours of the forecast, over-predicting rainfall by up to 14 times the observed. This indicates that there was still a model spin-up issue even with a hot-start initialization. Although the hot-start initialization should produce a fully balanced initial state, it is apparent that during this time the model was still trying to reach a state of equilibrium under the applied forcing. The LAPS-NMM configuration also spun up too much rainfall during this time. However, it had a smaller bias and only over-predicted rainfall by approximately three times the observed rainfall. All ADAS-ARW forecasts consistently over-predicted rainfall accumulation and failed to capture the late afternoon convective maximum. All LAPS-ARW forecasts also over-predicted accumulated rainfall. However, during the last six hours of the 1200 and 1500 UTC runs, the forecasted precipitation mirrored the observations more closely and the model captured the late afternoon convective maximum. The rainfall bias for the LAPS-NMM configuration was smaller than for both the ADAS-ARW and LAPS-ARW configurations. Nevertheless, not only did LAPS-NMM fail to capture the late afternoon convective maximum, the 1500 UTC run indicated a late afternoon minimum in convective activity. However, an increase in accumulated rainfall occurred after the late afternoon minimum indicating that the model may have just had a timing issue.

3.2 Fractions Skill Score in Space

Figure 5 shows the results from the calculation of FSS for all three model configurations. The calculation compared fractions from the models to the stage-IV precipitation analysis for five different spatial scales from the 4 km model grid scale to 160 km. Figure 6 shows the range of scales that the FSS was computed over using the shuttle launch pad at Launch Complex (LC) 39A as the center point. It is important to note that the score is more sensitive to small rain areas. Both ADAS-ARW and LAPS-ARW showed the least skill two hours after model initialization. This was consistent with the time of the maximum precipitation bias for both model configurations and was due to the model spin up process. Both model configurations showed some skill at predicting warm season convection in the 6 – 12 hour range over the spatial scales range of 40 to 160 km. However, the FSS on the grid scale of 4 km was consistently less than 0.4 throughout the forecasts for both ADAS-ARW and LAPS-ARW. The LAPS-NMM run showed little skill in the 2 – 5 hour range and the least skill overall. The FSS remained around 0.3 for the grid scale throughout the forecasts. For all configurations, model skill in forecasting the distribution of rainfall increased with spatial scale. Roberts (2005) noted that the skill should increase with spatial scale until it asymptotes at some value determined by the forecast bias. There were no significant differences in FSS between convection and non-convection days. In addition, prevailing wind direction (southeast, northeast, and east) did not produce significant differences in FSS.

Although there have been advances in forecast skill of numerical models for synoptic scale phenomena, warm season quantitative precipitation forecasts still pose a problem since the dynamics and thermodynamics of convection occur on the mesoscale and because our understanding of the cloud microphysics is limited (Fowle and Roebber 2003). Olsen et al (1995) found a threat skill score of less than 0.15 for a 25 mm threshold for warm season precipitation. Using no threshold value, the results here are slightly better, but still inadequate for producing an accurate precipitation forecast on the grid scale.

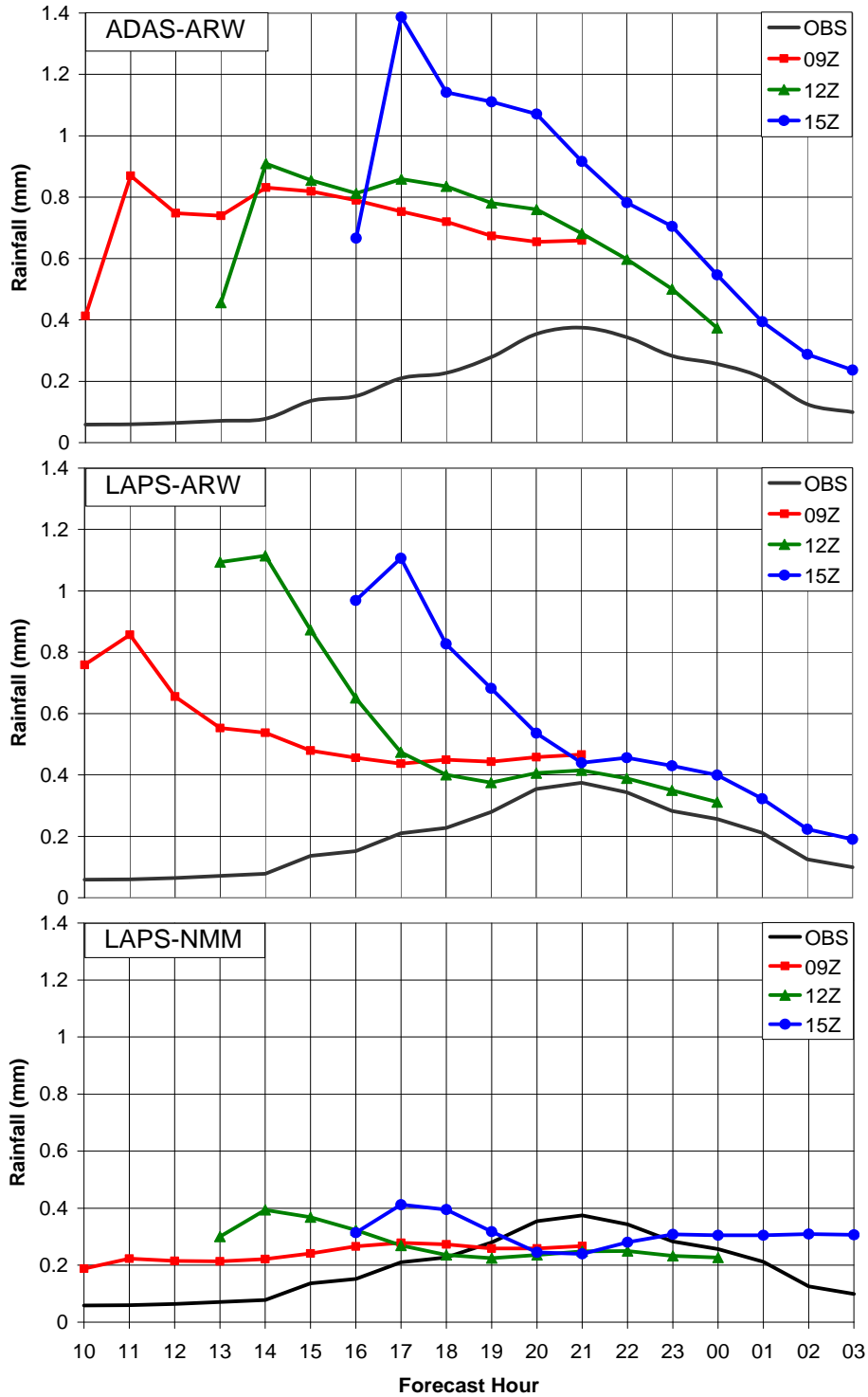


Figure 4. The forecast bias of rainfall accumulation (mm) versus time (UTC) for ADAS-ARW (top), LAPS-ARW (middle), and LAPS-NMM (bottom). The black line is the hourly observed rainfall accumulation averaged over the 4 km domain. The red, green, and blue lines are the averaged forecast rainfall accumulations for all model runs initialized at 0900, 1200, and 1500 UTC, respectively.

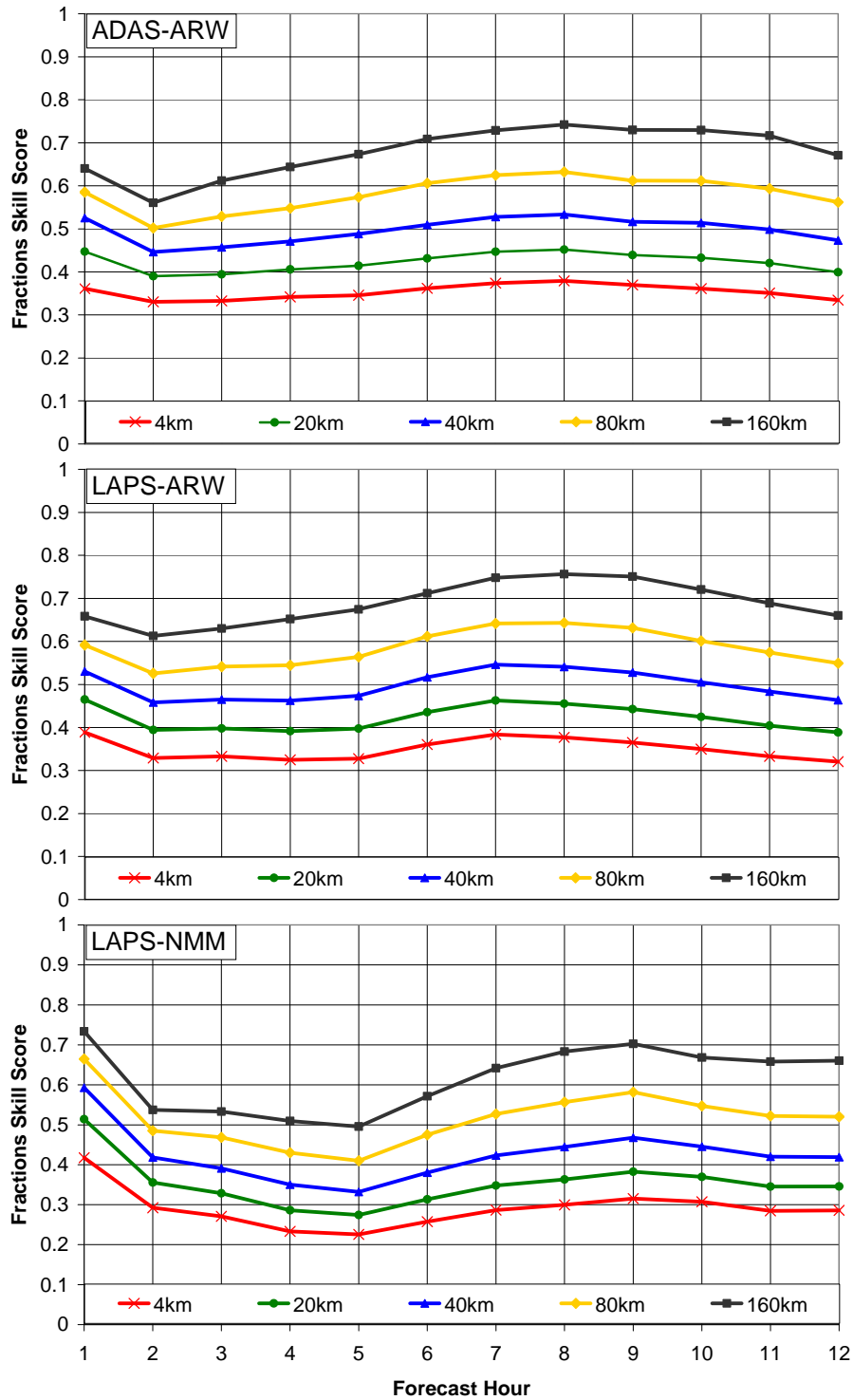


Figure 5. The Fractions Skill Score versus forecast hour for ADAS-ARW (top), LAPS-ARW (middle), and LAPS-NMM (bottom). The colored lines represent model skill on different spatial scales, from the grid scale at 4 km to 160 km. The color legend is on the bottom of each chart.

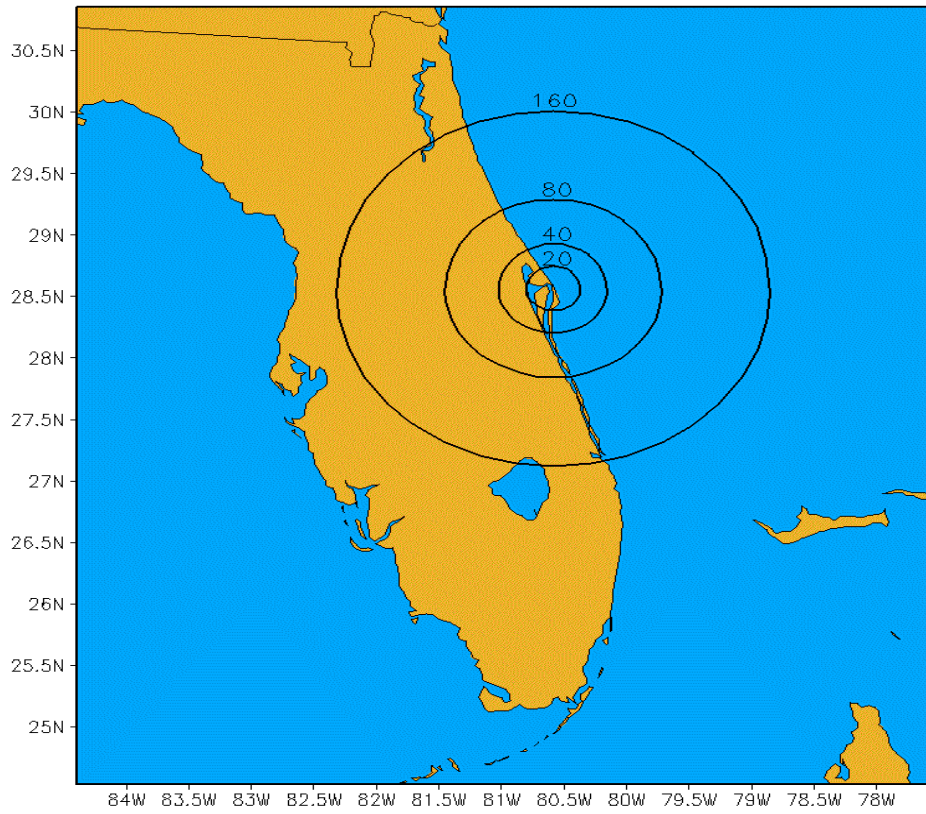


Figure 6. The range of spatial scales for the FSS calculations, starting from the grid scale at 4 km (center point) to 160 km. The center point of each circle is located at LC 39A.

3.3 Fractions Skill Score in Space and Time

To account for the timing of the convection, fractions for each grid square were computed as a function of the number of surrounding grid squares in space as well as time in which there was precipitation. Fractions in space can be thought of as a two-dimensional product (a function of x and y) while fractions in space and time can be thought of as a three-dimensional product (a function of x , y , and t). Fractions for the five different spatial scales and two temporal scales, one and two hours, were computed. The one-hour scale takes into account fractions one hour prior to and one hour after the current time. The two-hour scale takes into account fractions two hours prior to and after the current time.

Figure 7 shows the change in skill when the two temporal scales were taken into account over the same range of spatial scales as in Figure 5 for ADAS-ARW, LAPS-ARW, and LAPS-NMM. As expected, skill increased when the temporal scale was considered. The skill on the grid scale of 4 km increased the most with an approximate 25% increase in skill for the one-hour scale and an approximate 40% increase in skill for the two-hour scale. The rate of increase in skill was the largest moving inward from approximately 70 km to the grid scale. Moving from 180 to 70 km, the rate of increase in skill was small. The average difference in skill for all model configurations between the one- and two-hour scales was approximately 10%. The increase in skill was similar for the three model configurations at the 1-hour scale at all spatial scales. There was a higher increase in skill for the two-hour scales in each model, with the LAPS-NMM configuration showing a higher increase than the other two model configurations.

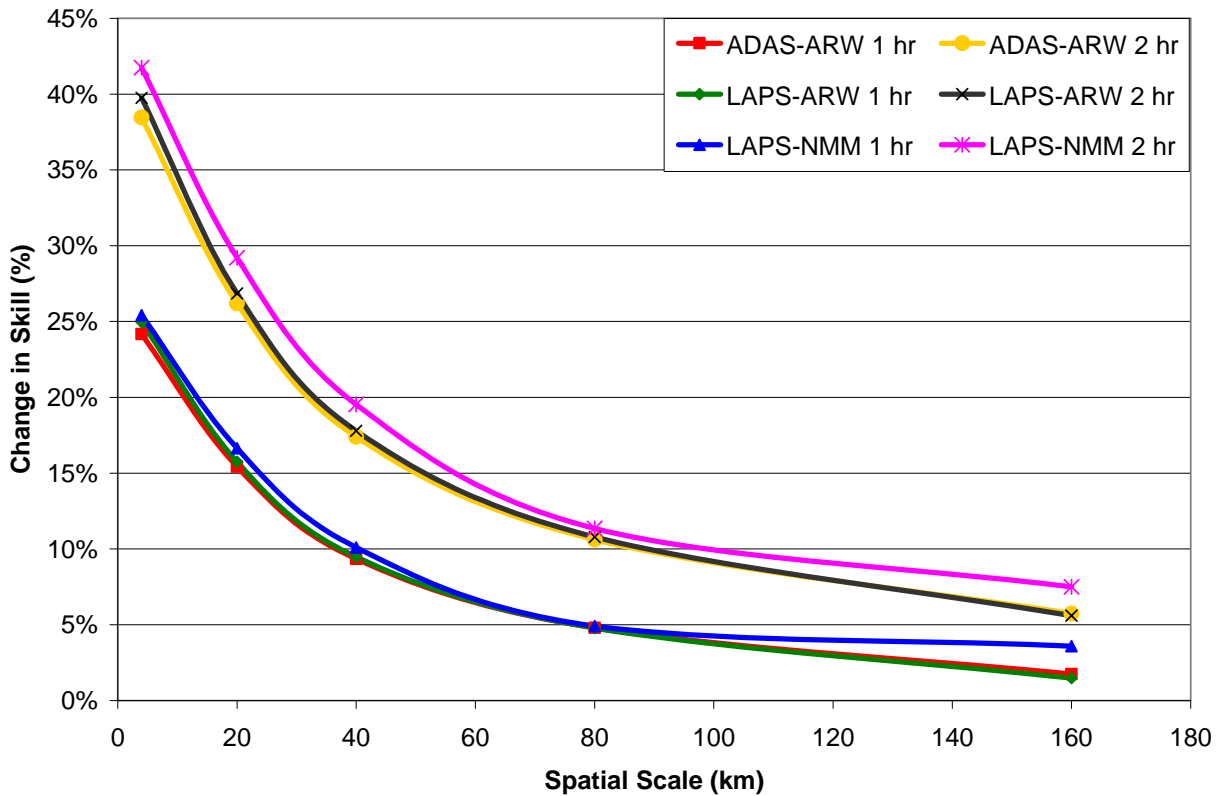


Figure 7. Change in skill when one- and two-hour temporal scales were taken into account for all three WRF model configurations over the range of spatial scales shown in Figure 6. The legend showing the color of each curve for each model and temporal scale combination is in the upper right.

3.4 Subjective Evaluation

Although FSS can illustrate the spatial and temporal skill of the model and can be used to compare model performance, it does not provide information regarding the nature of why the forecasts verified well or not. Similarly, forecast bias can tell which model over or under-predicted convection, but does not take into account whether the model produced widespread light rain or isolated heavy rain events. To help alleviate this issue, a subjective evaluation was employed. It should be noted that the 0-hour forecast composite reflectivity for all WRF initializations was nearly identical to the observations.

Figure 8 shows the observed composite reflectivity from all Florida WSR-88D radars valid at 1500 UTC 17 July 2006 and three-hour forecast composite reflectivity using ADAS-ARW, LAPS-ARW, and LAPS-NMM initialized at 1200 UTC 17 July 2006. Comparing the three-hour forecast of ADAS-ARW and LAPS-ARW to the observed composite reflectivity, it is evident that the forecast rain rate exceeded the observed rain rate and the model predicted too many rain areas over the waters surrounding the Florida peninsula. This is consistent with the large forecast bias and low skill during the initial stages of the forecast shown in Figure 4 and Figure 5, respectively. The LAPS-NMM configuration also over-predicted convection over the waters surrounding the Florida peninsula, however, the forecast rain rate was much smaller compared to the other two model configurations.

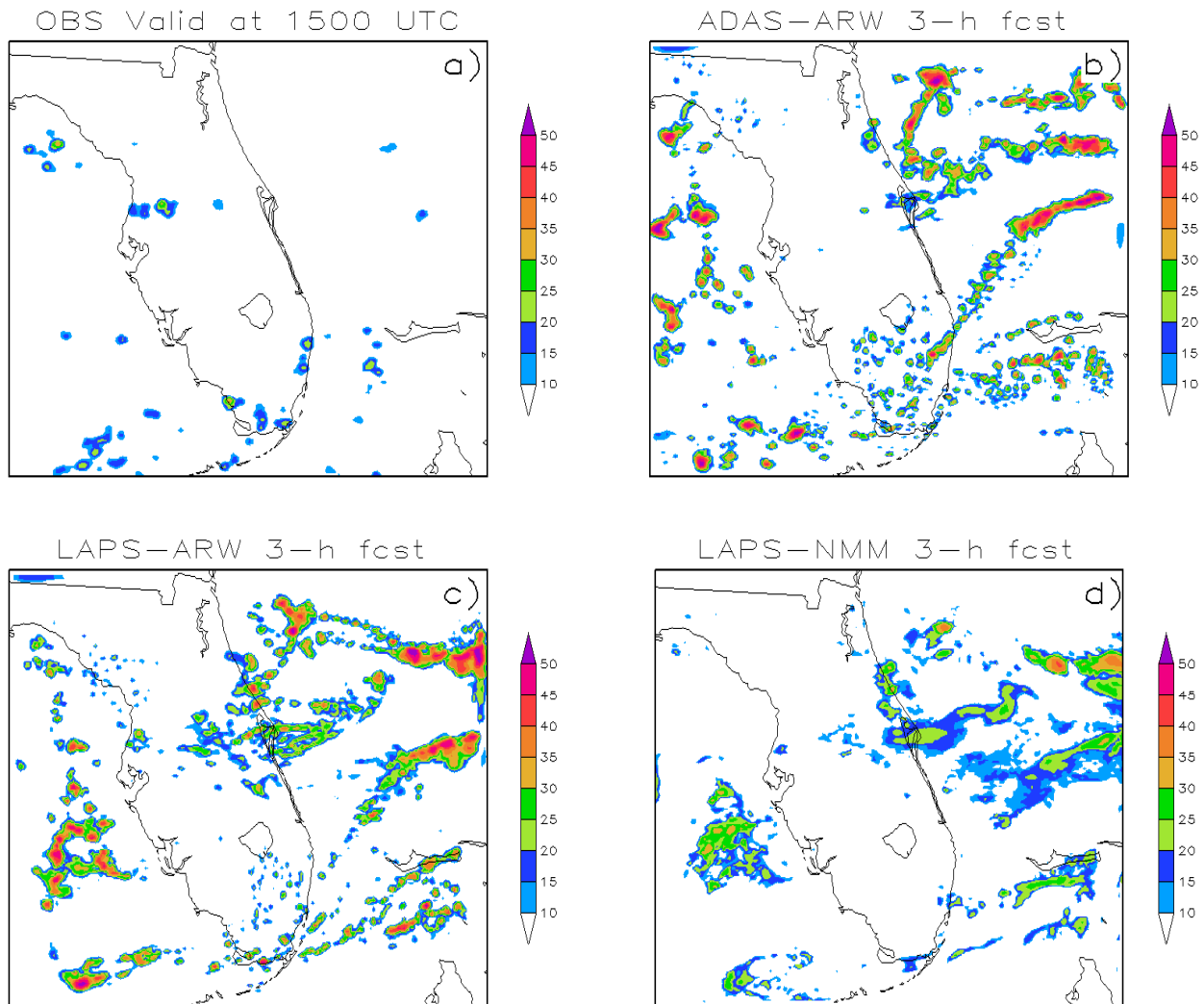


Figure 8. The a) observed composite reflectivity valid at 1500 UTC 17 July 2006 and b) ADAS-ARW, c) LAPS-ARW, and d) LAPS-NMM three-hour forecasts of composite reflectivity initialized at 1200 UTC 17 July 2006.

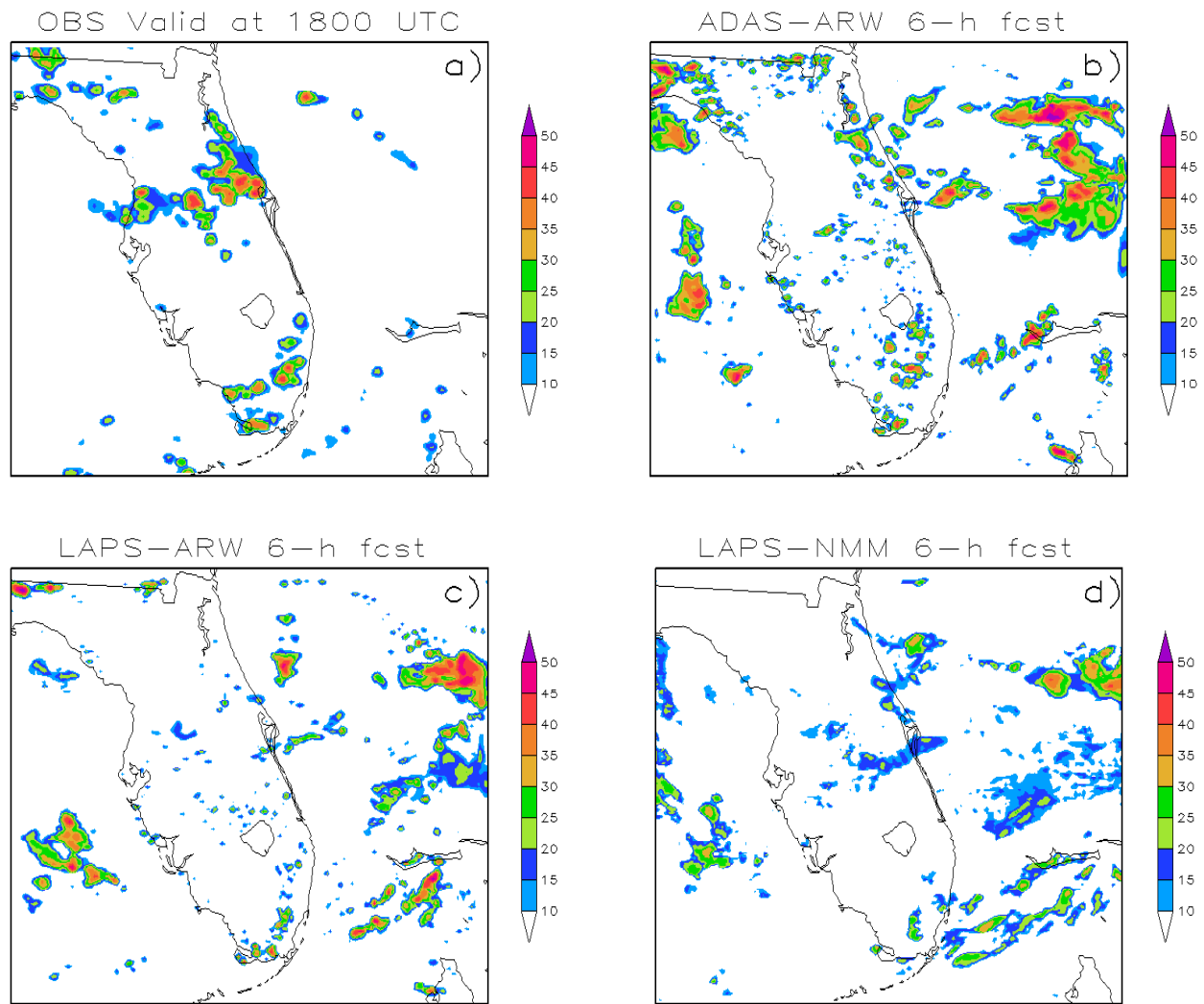


Figure 9. The a) observed composite reflectivity valid at 1800 UTC 17 July 2006 and b) ADAS-ARW, c) LAPS-ARW, and d) LAPS-NMM six-hour forecasts of composite reflectivity initialized at 1200 UTC 17 July 2006.

Figure 9 shows the observed composite reflectivity valid at 1800 UTC 17 July 2006 and six-hour forecast composite reflectivity using ADAS-ARW, LAPS-ARW, and LAPS-NMM initialized at 1200 UTC 17 July 2006. By 1800 UTC, the observations indicate a line of storms had developed across the central part of Florida from the Gulf of Mexico to the Atlantic Ocean. The ADAS-ARW and LAPS-ARW configurations failed to capture this phenomenon and continued to over-predict convection over the waters surrounding the Florida peninsula. However, it should be noted that the amount of convection produced by LAPS-ARW was less than the amount produced by ADAS-ARW. The LAPS-NMM configuration did forecast a line of convection extending from the CCAFS area west to central Florida, however, this line of convection was too weak and too far south as compared to the observations. As with ADAS-ARW and LAPS-ARW, LAPS-NMM also over-predicted convection over the ocean.

Figure 10 shows the observed composite reflectivity valid at 2100 UTC 17 July 2006 and nine-hour forecast composite reflectivity using ADAS-ARW, LAPS-ARW, and LAPS-NMM initialized at 1200 UTC 17 July 2006. By 2100 UTC convection was occurring across northern and central Florida and along the southeast Florida coast. The nine-hour ADAS-ARW and LAPS-ARW composite reflectivity reveals rain rates that are too strong and indicated widespread convection across the Florida peninsula, not centered around central Florida as seen in the observations. At this time, the convection across south Florida was too far inland, suggesting that the model had pushed the sea breeze too far inland at this time. Convection also remained over the waters east of the peninsula, which was not in the observations. The LAPS-NMM configuration failed to capture the intense area of convection across north and central Florida. There was no evidence of sea breeze formation and too much convection over the waters east of the peninsula.

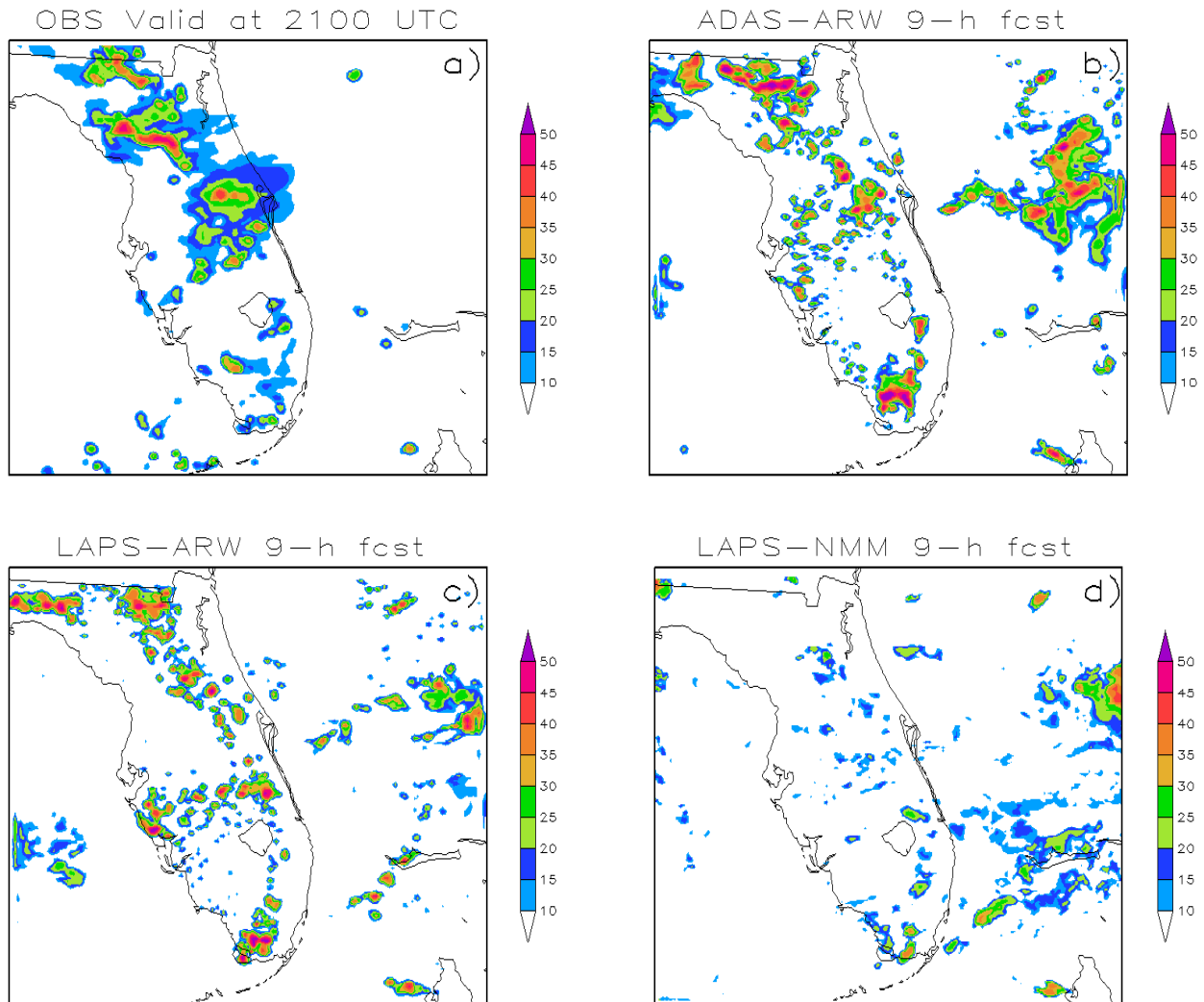


Figure 10. The a) observed composite reflectivity valid at 2100 UTC 17 July 2006 and b) ADAS-ARW, c) LAPS-ARW, and d) LAPS-NMM nine-hour forecasts of composite reflectivity initialized at 1200 UTC 17 July 2006.

Figure 11 shows the observed composite reflectivity valid at 0000 UTC 18 July 2006 and 12-hour forecast composite reflectivity using ADAS-ARW, LAPS-ARW, and LAPS-NMM initialized at 1200 UTC 17 July 2006. At this time, the observations indicate convection remaining over north Florida and forming along the west coast of Florida. By hour 12, both the ADAS-ARW and LAPS-ARW forecasts more closely resembled the observed composite reflectivity showing convection over north Florida that spread down the west coast. However, rain rates were far too strong. The LAPS-NMM configuration started to develop convection across north central Florida at this time, which may indicate that the model had a timing issue.

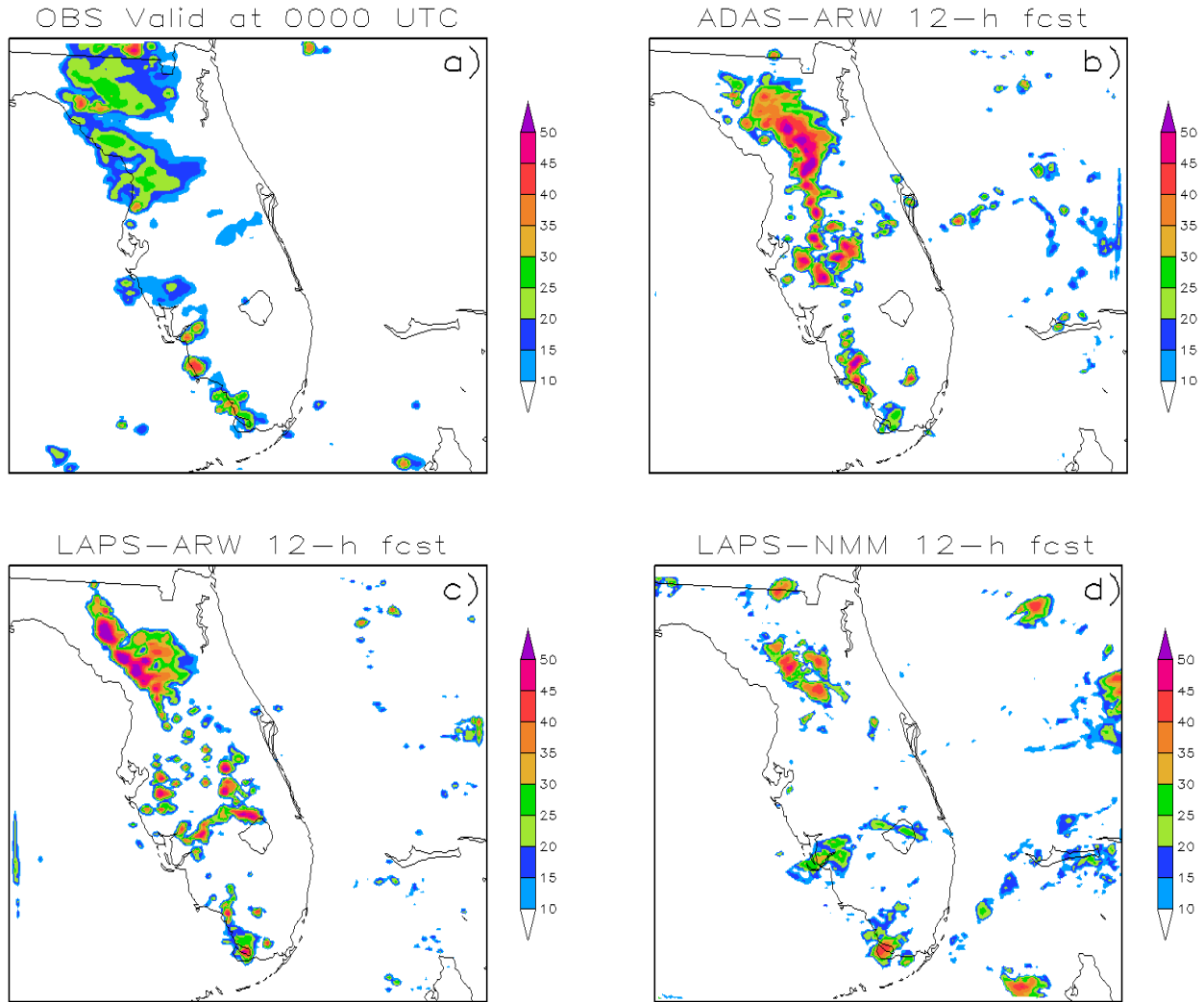


Figure 11. The a) observed composite reflectivity valid at 0000 UTC 18 July 2006 and b) ADAS-ARW, c) LAPS-ARW, and d) LAPS-NMM 12-hour forecasts of composite reflectivity initialized at 1200 UTC 17 July 2006.

Overall, all model configurations did a poor job of representing convection for all candidate days. Prevailing wind direction did not seem to have an impact on the subjective skill of the model. Because these convective episodes occur on the mesoscale, these results are perhaps not too surprising. Fowle and Roebber (2003) found that errors can occur in three different ways: 1) sensitivity to initial conditions, 2) choice of cumulus parameterization scheme, and 3) understanding of precipitation processes in general. Cumulus parameterization issues would not factor into these results since no convective parameterization schemes were used. Jankov et al. (2005) found that the microphysical scheme could have a considerable impact on the total rain volume while Gallus and Bresch (2006) found that total rain volume is more sensitive to the choice of dynamic core. In their study, they found some indication that the NMM runs were drier than the ARW runs. These results are in agreement as both ARW runs over-predicted rain amounts throughout the domain, while the NMM core was drier. The choice of LAPS or ADAS

for the initial condition did not seem to impact the forecast. Each produced an accurate initial condition as far as location of convection and produced a similar overall forecast when using the same dynamic core. In fact, Gallus and Bresch (2006) found that the impact of changes in the initial condition was generally smaller than the impact of changes in the dynamic core or physics.

4. Comparison of Nesting Options

Due to limitations in the NMM core, only the ARW core could be used for nested model runs. The LAPS-ARW configuration was chosen based on a comparison of results from the 4 km ADAS-ARW and LAPS-ARW model runs. Although the objective analysis for both models was similar, a subjective verification suggested the LAPS-ARW configuration slightly outperformed the ADAS-ARW. Each nested fine-mesh inner grid for the one- and two-way nested configurations covered the east-central Florida region and had a grid spacing of 1.33 km (Figure 2). The no nesting option is simply a 4 km grid subset over east-central Florida. A comparison of hourly model rainfall accumulation to stage-IV rainfall accumulation analyses was made for each forecast for all convection days for each of the nesting options. The stage-IV data was averaged to the same grid as the high-resolution nested domain to give a similar comparison. In addition to assessing the spatial and temporal accuracy of the different nesting options, the forecast bias was also examined.

4.1 Forecast Bias

Figure 12 shows the forecast bias for the LAPS-ARW nest using one-way, two-way, and no nesting. The forecasts from the 0900 and 1200 UTC runs were similar for both the one- and two-way nesting configurations. Both nesting configurations over-predicted precipitation during the initial stages of the forecast, exhibiting the same model spin up problem as was seen with the 4 km runs. They capture the timing of the late afternoon convective maximum, although both under-predicted the rainfall during this time by approximately 0.4 mm (.02 in). The no-nest run also over-predicted rainfall over the local domain at the start of both the 0900 and 1200 UTC runs, but then captured the timing of the late afternoon convective maximum and the correct amount of rainfall.

The timing of the late afternoon convective maximum in the 1500 UTC runs of all nesting configurations was delayed by approximately three hours. The one-way nest exhibited two peaks in rainfall, one at 1900 UTC and another at 2300 UTC. The two-way nested 1500 UTC run accurately captured the trend in rainfall accumulation, however, it under-predicted the amount of precipitation. The no nesting run over-predicted the afternoon convective maximum by approximately 0.3 mm (.01 in).

4.2 Fractions Skill Score in Space

Figure 13 shows the results from the calculation of FSS for all three nesting configurations. This compares fractions from the forecasts to the stage-IV precipitation analyses averaged over the model domain for five different spatial scales as stated in Section 2.5: from the model grid scale of 1.33 km to 53.2 km. Figure 14 shows the range of scales that the FSS was computed over using LC 39A as the center point. The FSS of all three nesting configurations look nearly identical with low skill in the 0.3 – 0.4 range during the first few hours, increasing to 0.4 – 0.6 in the last five hours, with peak skill in the 8-hour forecast. Each configuration increased in forecast skill by nearly 50% from the first six hours of the forecast to the last six hours. This suggests that the model still had a problem with spin up even when running at a higher resolution on a smaller domain. The FSS for the two-way nested run was approximately 0.5 less than those for the one-way and no nest runs. As with the different WRF initializations, the skill of the model in forecasting the distribution of rainfall increased with spatial scale, however, the difference in skill between scales was smaller for the nesting configurations than for the different WRF initializations.

4.3 Fractions Skill Score in Space and Time

As with the three model configurations, the FSS was calculated for the temporal scale as described in Section 3.3. The method of computation is the same as for the different WRF configurations, except that the scale sizes were different. Figure 15 shows the change in skill (in %) when temporal variability was taken into account over a range of spatial scales for one-way, two-way, and no nesting. The skill increased for all nesting configurations except for the no-nest one-hour scale at 1.33 km, which had a 5% decrease in skill. For all nesting configurations, the most skill was gained at 7 km, ranging from an 18 – 36% increase in skill. For scales larger than 7 km, the skill decreased by 2 - 9%. The no-nesting one-hour scale gained the least skill while the two-way nested two-hour scale gained the most skill.

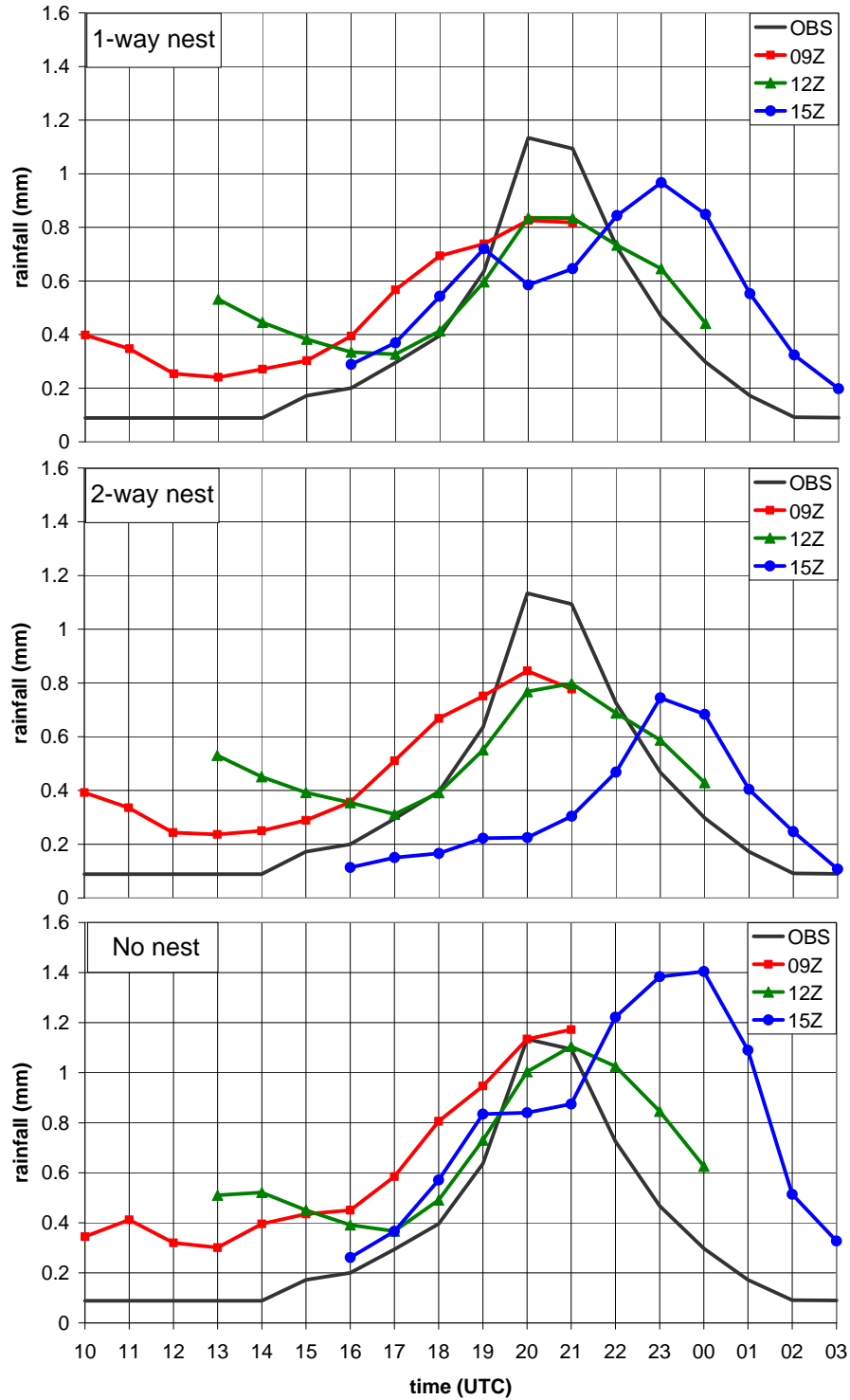


Figure 12. The forecast bias of rainfall accumulation (mm) versus time (UTC) for LAPS-ARW 1.33 km nest using one-way (top), two-way (middle), and no nesting (bottom). The black line is the hourly observed rainfall accumulation averaged over the 1.33 km domain. The red, green, and blue lines are the averaged forecast rainfall accumulations for all model runs initialized at 0900, 1200, and 1500 UTC, respectively.

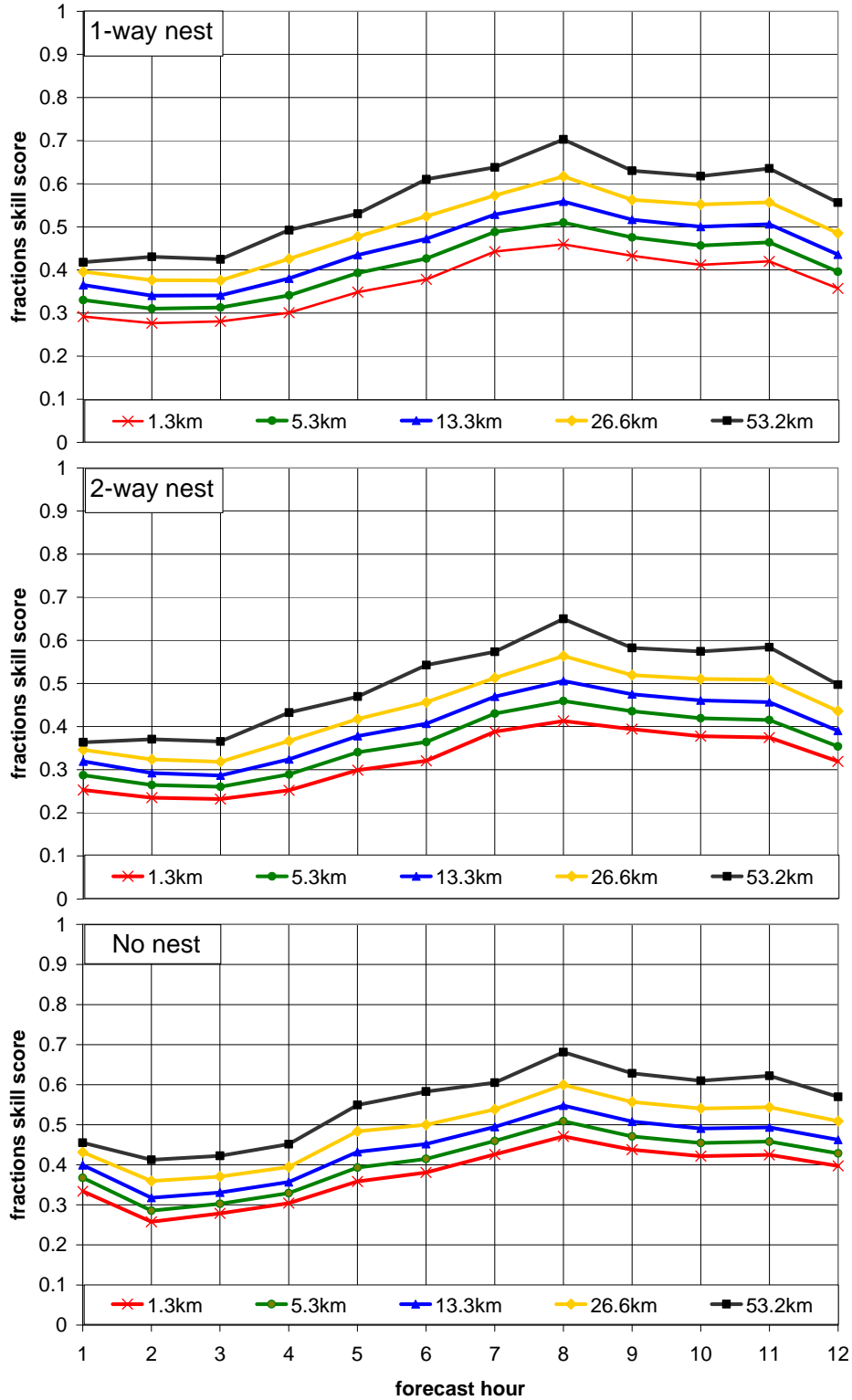


Figure 13. The Fractions Skill Score versus forecast hour for LAPS-ARW 1.33 km nest using one-way (top), 2-way (middle), and no nesting (bottom). The colored lines represent model skill on different spatial domains, from the grid scale of 1.33 km to 53.2 km. The color legend is on the bottom of each chart.

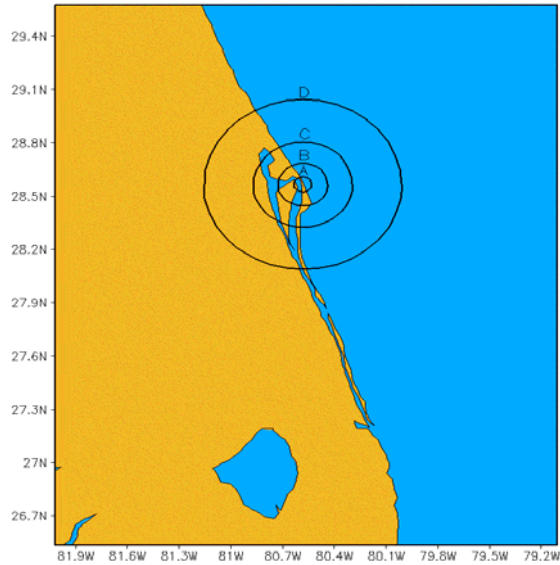


Figure 14. Range of spatial scales FSS was computed over for the 1.33 km nested runs. Circle A represents 5.3 km, B represents 13.3 km, C represents 26.6 km, D represents 53.2 km. The center point of each circle, which represents the grid scale, is located at LC 39A.

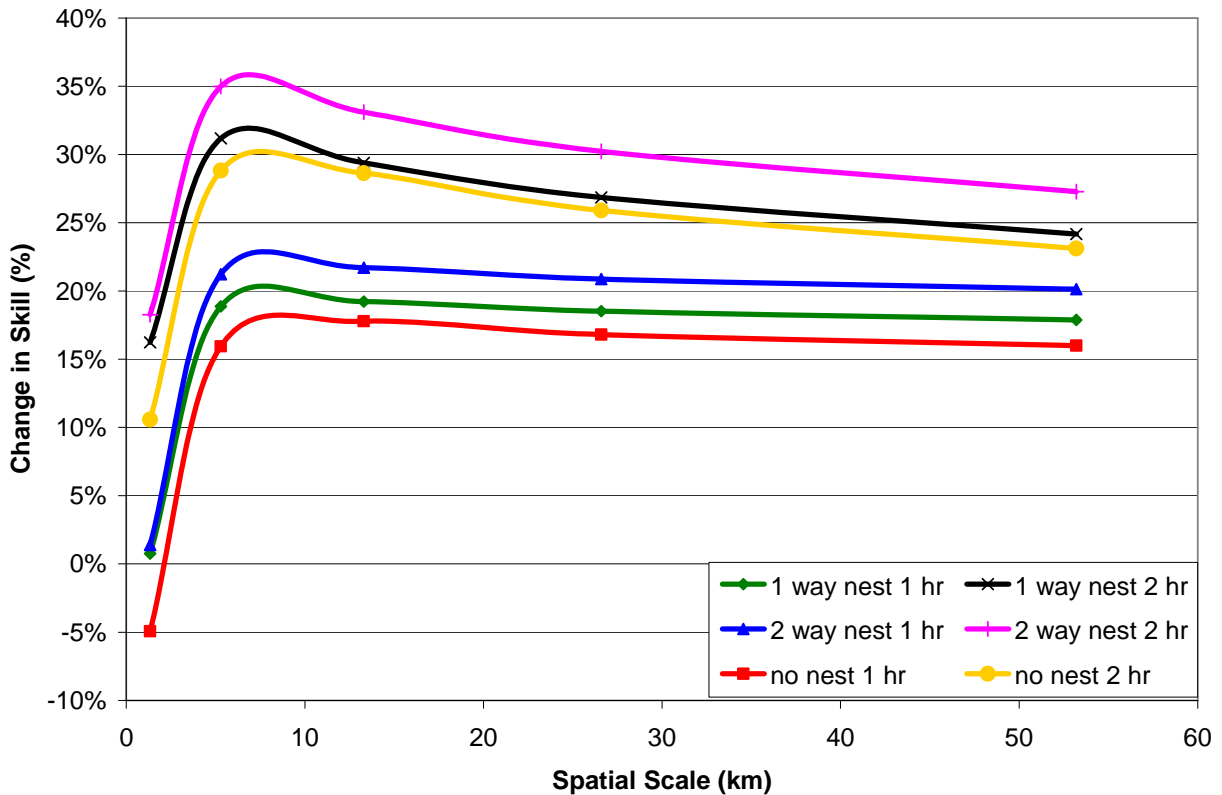


Figure 15. Change in skill when one- and two-hour temporal scales were taken into account for all three LAPS-ARW nesting configurations over the range of spatial scales shown in Figure 14. The legend showing the color of each curve for each model and temporal scale combination is in the lower right.

4.4 Subjective Evaluation

Observed and three-hourly forecasts of composite reflectivity from a 12-hour forecast using one-way, two-way, and no nesting initialized at 1200 UTC 17 July 2006 are shown in Figure 16, Figure 17, Figure 18, and Figure 19. Examination of the forecast reflectivity in all figures for the one- and two-way nested runs reveals they were nearly identical. In addition, the 0-hour forecast composite reflectivity for all nesting configurations was nearly identical to the observations. The no-nested run resembled the one- and two-way nested runs without the fine-scale resolution.

Indicated in Figure 16, as with the three WRF initializations, the nested runs spun up too much convection in the forecast domain by 1500 UTC. At 1800 UTC (Figure 17), the observed composite reflectivity showed an area of heavy precipitation over the northwest corner of the model domain (northern Brevard and Volusia counties). All nesting configurations did capture this area of storms, but mislocated it to the northeast. In addition, the models developed too many convective cells throughout the forecast domain. By 2100 UTC (Figure 18), strong storms covered most of Brevard, Volusia, and counties to the west. At this time, all configurations failed to capture the extent of these storms and instead forecast widespread convection across the domain. Also, all configurations showed convective initiation ahead of a sea breeze front which is not apparent in the observed composite reflectivity. By 0000 UTC (Figure 19), the nesting configurations still indicated strong areas of convection southeast of KSC/CCAFS, while the observed composite reflectivity indicated the dissipation of convection throughout the forecast domain.

Based on the subjective evaluation of this convective initiation event, it is apparent that the use of a high-resolution nested grid gave a more realistic structure to the individual storms, but did not resolve areas of convection that the coarser resolution run also failed to do. Also, the use of a nested run did not improve the skill of the model as it still had a problem with placement of convection.

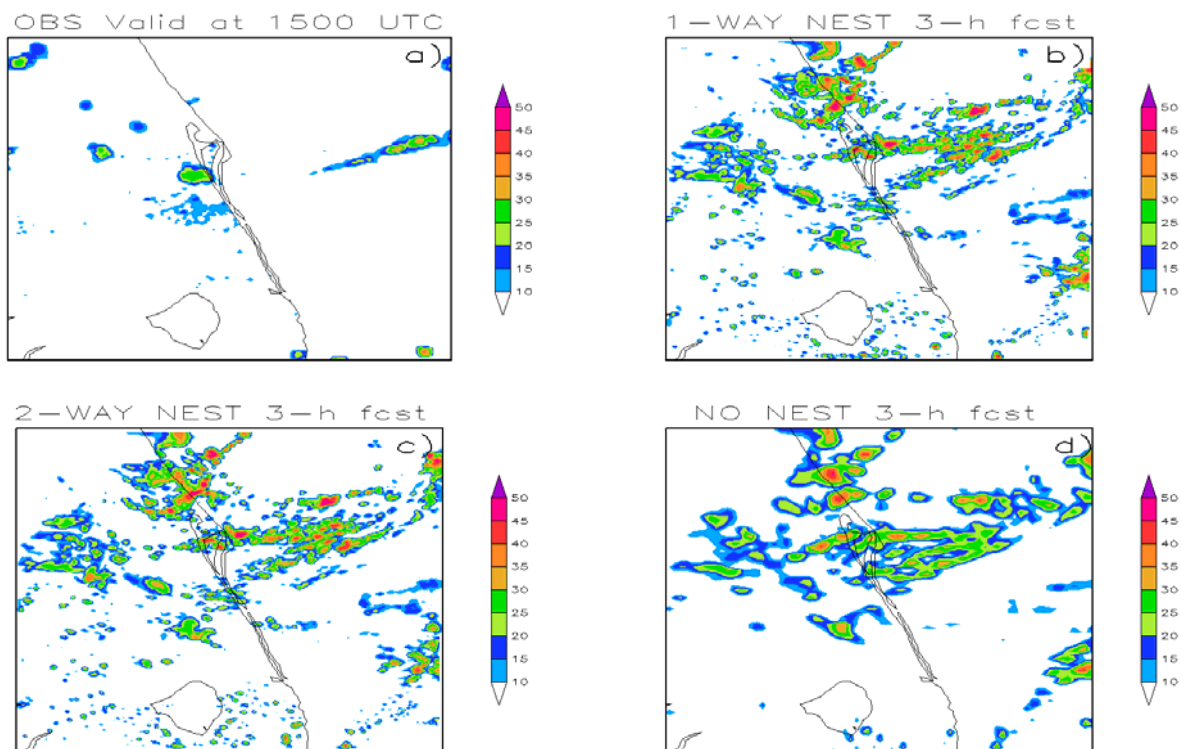


Figure 16. The a) observed composite reflectivity valid at 1500 UTC 17 July 2006 and b) 1-way, c) 2-way, and d) no nesting three-hour forecasts of composite reflectivity initialized at 1200 UTC 17 July 2006.

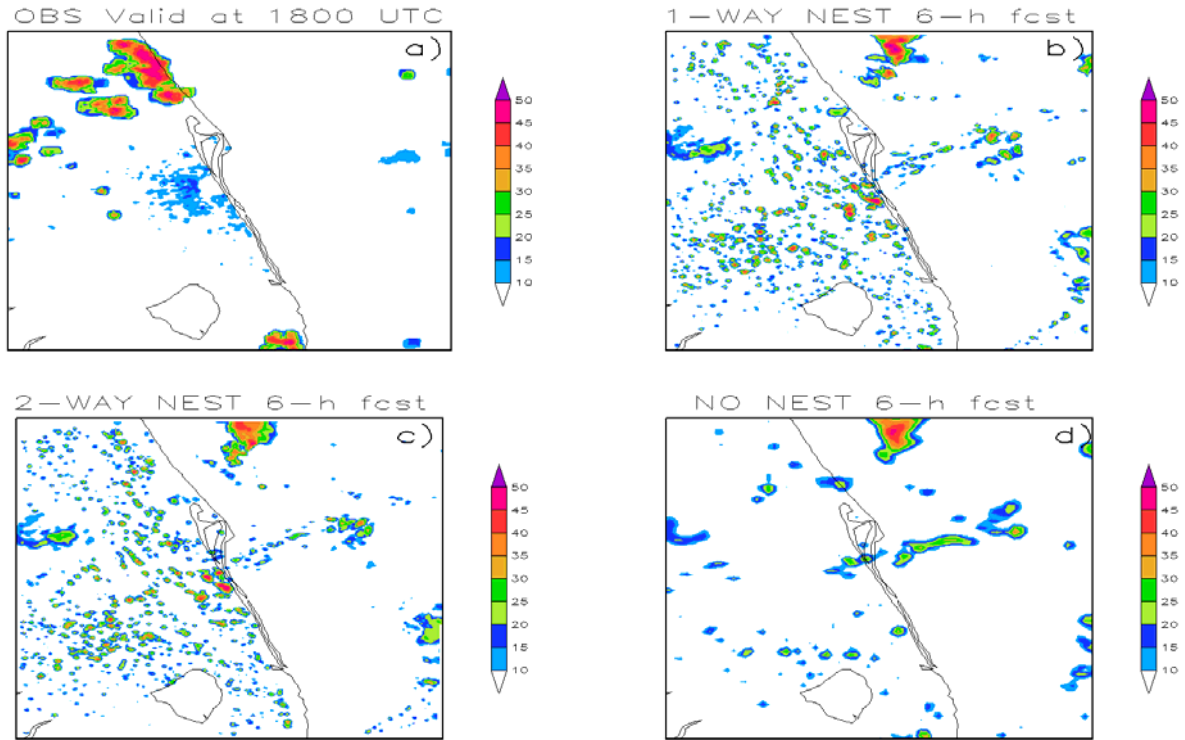


Figure 17. The a) observed composite reflectivity valid at 1800 UTC 17 July 2006 and b) 1-way, c) 2-way, and d) no nesting six-hour forecasts of composite reflectivity initialized at 1200 UTC 17 July 2006.

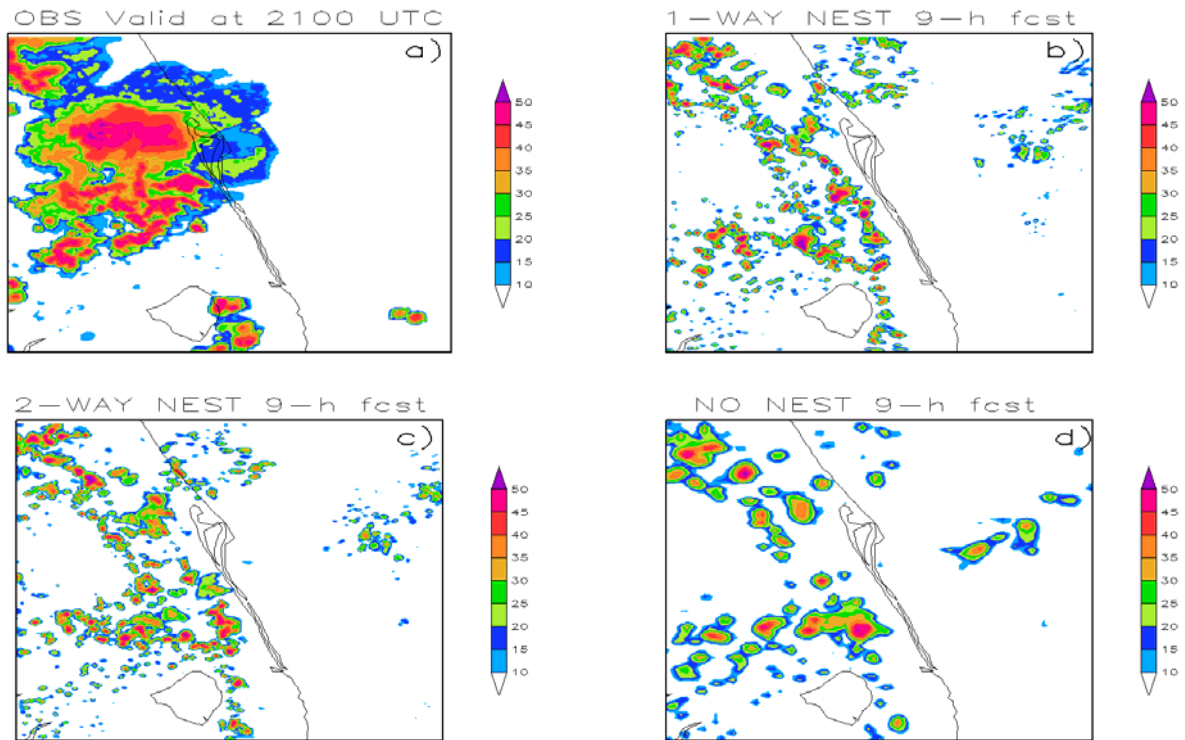


Figure 18. The a) observed composite reflectivity valid at 2100 UTC 17 July 2006 and b) 1-way, c) 2-way, and d) no nesting nine-hour forecasts of composite reflectivity initialized at 1200 UTC 17 July 2006.

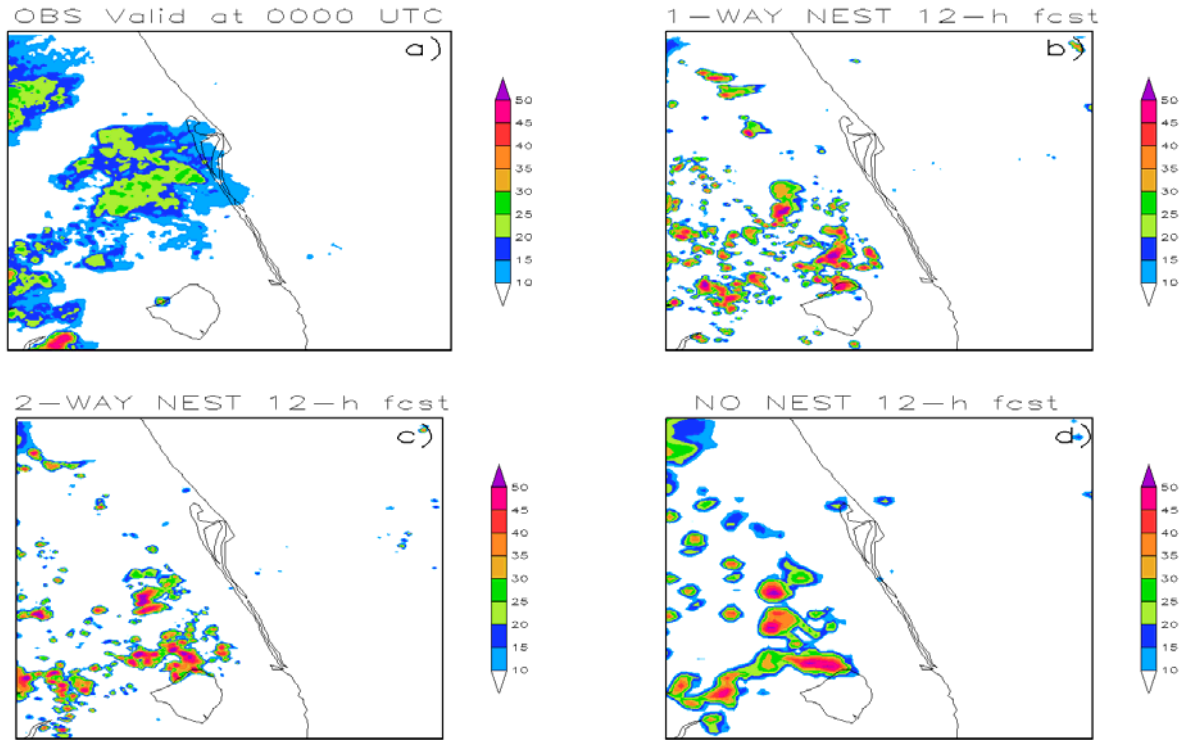


Figure 19. The a) observed composite reflectivity valid at 0000 UTC 18 July 2006 and b) 1-way, c) 2-way, and d) no nesting 12-hour forecasts of composite reflectivity initialized at 1200 UTC 17 July 2006

5. Soil Moisture Assimilation

As mentioned in Section 2.4, neither LAPS nor ADAS can assimilate and analyze in-situ soil moisture data into their analyses, therefore, the impact of assimilating soil moisture sensor data on WRF model performance could not be completed as required by the task. Rather, a description of alternative methods for ingesting soil moisture data into the WRF model is presented here.

As mesoscale models increase in resolution, it is becoming more important to initialize the model in order to capture the small scale features that are forced by the ground surface. Land surface models (LSMs) serve this purpose by producing estimates of soil moisture and temperature, evapotranspiration, and other fluxes of water and energy (Rodell et al. 2005). A number of LSMs have been developed recently such as NCEP's Community Noah Land Surface Model (NOAH), NCAR's Community Land Model (CLM), NASA's Land Information System (LIS), and University of Washington's Variable Infiltration Capacity (VIC) model. These LSMs can be run in either of two ways: off-line or coupled with a numerical weather prediction model. In the off-line strategy, the LSM is forced with meteorological data while assimilating observations of land surface fields (Reichle 2005). In this case, there is no feedback between the land surface forcing and the atmospheric state. In a coupled system, land assimilation is performed in conjunction with the atmospheric analysis such that there is consistency between the initial land and atmospheric states. This is more computationally demanding to run than an off-line LSM.

Since LAPS and ADAS cannot currently assimilate soil moisture data, a land data assimilation system (LDAS) that blends the observations with the background fields of the LSMs is needed (Mitchell et al. 2003). Currently, there is a joint collaboration between several NASA and the National Oceanic and Atmospheric Administration (NOAA) agencies and universities, called the Land Data Assimilation Scheme (LDAS) Project, whose goal is to develop an LDAS consisting of uncoupled models forced with observations (Cosgrove et al. 2003). For example, one part of this study called the North American LDAS (NLDAS), produces hourly surface forcing using model-independent, observation-based precipitation and insolation fields that drives four LSMs running in parallel. This NLDAS generates hourly output over a CONUS domain (Lohmann et al. 2005). These data can then be incorporated into a local numerical weather prediction model. Only the NLDAS data is presently available, not the source code needed to ingest local soil moisture data.

Currently, the use of an LDAS is the only way to incorporate soil moisture data into the WRF model, until the LAPS soil moisture algorithm is fully developed. One LDAS that is available to the public right now is NASA's LIS. This system runs several different LSMs in an uncoupled manner using model and observational input, including precipitation and many surface parameters (Kumar et al. 2006). There are two components to the LIS software: a driver and the LSMs. The LIS driver is the core that controls the different offline LSMs (Peters-Lidard et al. 2004). The LIS system currently includes NCAR's CLM, NCEP's NOAH, and University of Washington's VIC model (Kumar et al. 2006). Running an off-line high-resolution LSM is a significant computational effort. However, the LIS software has been redesigned to reduce the computational demand (Peters-Lidard et al. 2004).

6. Conclusions

The evaluation described in this report was designed to assess the skill of the three different hot-start model configurations of the WRF model and the different nesting options available for forecasting warm season convective initiation. A total of seven candidate days were chosen to assess model skill. To compare the three different combinations of WRF initializations, ADAS-ARW, LAPS-ARW, and LAPS-NMM, the WRF model was run for 12 hours, three times a day, at a 4 km horizontal grid spacing over the Florida peninsula. Data ingested by the model through the data analysis packages included WSR-88D data, satellite imagery, and surface observations throughout Florida. To compare the performance of the WRF model using a high-resolution local grid with one-way, two-way, and no nesting, the inner nest was run with a grid spacing of 1.33 km over east-central Florida. The objective verification of the model focused on the overall accuracy of precipitation forecasts across the Florida peninsula and the surrounding coastal waters, as well as the local east-central Florida region. While a study of the full convective season would be ideal, it was felt that using a handful of representative days would help in obtaining an overall view of the skill of each model configuration.

6.1 Results

The major results from the evaluation show the following.

- During the model spin up process, too much precipitation developed across the forecast area for both ADAS-ARW and LAPS-ARW.
- ADAS-ARW and LAPS-ARW over-predicted rainfall amounts across Florida and the surrounding coastal waters throughout the 12-hour forecast.
- As the forecast progressed, the rainfall bias decreased and the skill increased indicating that all models performed better beyond six hours.
- The difference in skill between the ADAS-ARW and LAPS-ARW was negligible, while the skill of LAPS-NMM was slightly worse.
- Based on a subjective analysis of the three WRF initializations, LAPS-ARW slightly outperformed the other two configurations.
- The skill of each WRF initialization and nesting configuration increased as the spatial scale increased and when accounting for temporal variability.
- Both one- and two-way nesting configurations under-predicted the late afternoon convective maximum over east-central Florida.
- As with the three hot-start model configurations, the skill of the forecasts for the different nesting configurations increased as the forecast progressed.
- The difference in skill between the 1-way, 2-way, and no nest configurations was negligible.
- The use of a local high-resolution grid did not significantly improve the skill of the model as compared to the 4 km model runs.

The analysis of all hot-start model configurations and nesting configurations indicated that no single model was clearly better than the rest. However, overall LAPS-ARW and ADAS-ARW did outperform LAPS-NMM. Although the NMM core runs faster than the ARW core (approximately 1.6 times faster using a 3.2-GHz cluster with 48 processors), it has a dry bias and fails to capture areas of heavy precipitation. The post-processing for the NMM core also takes longer. However, this can be mitigated by reducing the number of variables output. It is important to note that these results are limited in scope by the number of candidate days chosen.

The information from this study can be used to determine the smallest spatial scales over which model output is presented. If an FSS of 0.5 is deemed acceptable to the user, precipitation output from a LAPS-ARW run represents scales of around 60 km during the first 5-6 hours of the forecast and about 30 km during hours 6-12. That is, when running the model with 4 km grid spacing, precipitation can be expected within 60 km of the forecast location during hours 0-6 and within 30 km during hours 6-12. These results suggest that high-resolution forecasts over

Florida during the warm season are best to help develop a broad understanding of a situation rather than in predicting individual convective cells.

6.2 Recommendations

Of the three model configurations tested, the AMU recommends the LAPS-ARW configuration for operational use for predicting warm season convective initiation for the following reasons:

- Although the FSS values for the LAPS-ARW and ADAS-ARW forecasts were nearly identical, LAPS-ARW appeared to over-predict the precipitation less than the ADAS-ARW over the domain;
- The LAPS-NMM configuration produced forecasts that were too dry;
- The ADAS does not have the capability to assimilate soil moisture data, but a soil moisture algorithm may be developed for LAPS; and
- The challenge of setting up the LAPS software can be avoided by using LAPS analyses from the Advanced Weather Interactive Processing System (AWIPS) for use within the WRF EMS software, eliminating the need for running an outside analysis before running the WRF model.

The AMU is not recommending any one of the three nesting configurations for operational use. The results in this study showed that the one-way, two-way, and no nest configurations produced output that was nearly identical.

The AMU believes that it is possible to improve local model convective initiation forecasts by improving soil moisture input through the use of an LSM that incorporates local soil moisture observations. An LSM can be run in real-time by acquiring real-time atmospheric forcing datasets such as the Global Data Assimilation System (GDAS) analyses, running the LSM offline, and restarting the LSM integration each day using the previous day's soil state.

6.3 Possible Future Work

A more robust analysis of scientific data and technology should be completed to address the issue of value of local model output for real-time decision making and to fully determine an optimized operational solution for convective initiation precipitation forecasts. The first step is to increase the number of convective initiation days used in the study, such as analyzing a full convective season. This will result in a more comprehensive representation of model skill for forecasting convective initiation. In addition, there are a few related tasks that the AMU could complete as an extension of this task. The first is to explore the use of either an offline or coupled LSM/WRF model. This has the capability of improving convective initiation forecasts by improving the land surface exchange processes, which have a direct effect on forecasts of clouds and precipitation. As mentioned, such a system can be run operationally. The second is to explore the use of ensemble modeling. This appears to be the direction in which the modeling community is moving based on recent findings in the literature and current research within the modeling community. However, problems still linger for forecasting convection even with the use of ensembles. Finally, a comparison of different model initial and boundary conditions could be explored to determine which is best for forecasting warm season convective initiation. In particular, a task to determine whether there is an improvement in forecasting convection by using high-resolution, WRF model output from a previous successive run as the initial and/or boundary conditions for the next run would be beneficial.

References

- Albers, S. C., 1995: The LAPS wind analysis. *Wea. Forecasting*, **10**,342–352.
- Albers, S. C., J. A. McGinley, D. L. Birkenheuer, and J. R. Smart, 1996: The Local Analysis and Prediction System (LAPS): Analyses of clouds, precipitation, and temperature. *Wea. Forecasting*, **11**, 273–287.
- Benjamin, S. G., J. M. Brown, K. J. Brundage, B. E. Schwartz, T. G. Smirnova, T. L. Smith, and L. L. Morone, 1998: RUC-2 – The Rapid Update Cycle Version 2 Technical Procedures Bulletin. NOAA Technical Procedures Bulletin. Retrieved from <http://maps.fsl.noaa.gov/>.
- Birkenheuer, D., 1999: The effect of using digital satellite imagery in the LAPS moisture analysis. *Wea. Forecasting*, **14**, 782–788
- Brewster, K., 1996: Implementation of a Bratseth analysis scheme including Doppler radar. Preprints, *15th Conf. on Weather Analysis and Forecasting*, Norfolk, VA, Amer. Meteor. Soc., 92–95.
- Brewster, K., 2002: Recent advances in the diabatic initialization of a non-hydrostatic numerical model. *Preprints, 15th Conf on Numerical Weather Prediction and 21st Conf on Severe Local Storms*, San Antonio, TX, Amer. Meteor. Soc., J6.3.
- Case, J., 1999: Simulation of a real-time Local Data Integration System over east-central Florida. NASA Contractor Report CR-1999-208558, Kennedy Space Center, FL, 46pp.
- Case, J. L., J. Manobianco, T. D. Oram, T. Garner, P. F. Blottman, and S. M. Spratt, 2002: Local Data Integration over East-Central Florida Using the ARPS Data Analysis System. *Wea. Forecasting*, **17**, 3-26.
- Chen, F., and J. Dudhia, 2001: Coupling an advanced land-surface/ hydrology model with the Penn State/ NCAR MM5 modeling system. Part I: Model description and implementation. *Mon. Wea. Rev.*, **129**, 569–585.
- Chou M.-D., and M. J. Suarez, 1994: An efficient thermal infrared radiation parameterization for use in general circulation models. NASA Tech. Memo. 104606, 3, 85pp.
- Cosgrove, B. A., D. Lohmann, K. E. Mitchell, P. R. Houser, E. F. Wood, J. C. Schaake, A. Robock, J. Sheffield, Q. Duan, L. Luo, R. W. Higgins, R. T. Pinker, and J. D. Tarpley, 2003: Land surface model spin-up behavior in the North American Land Data Assimilation System (NLDAS), *J. Geophys. Res.*, **108**(D22), 8845, doi:10.1029/2002JD00331603.
- Droegemeier, K. K., and R. B. Wilhelmson, 1985: Three-dimensional numerical modeling of convection produced by interacting thunderstorm outflows. Part I: Control simulation and low-level moisture variations. *J. Atmos. Sci.*, **42**, 2381–2403.
- Fels, S. B., and M. D. Schwarzkopf, 1975: The simplified exchange approximation: A new method for radiative transfer calculations. *J. Atmos. Sci.*, **32**, 1475-1488.
- Fovell, Robert G., 2005: Convective initiation ahead of the sea-breeze front. *Mon. Wea. Rev.*, **133**, 264-278.
- Fowle, M.A. and P.J. Roebber, 2003: Short-range (0-48 h) numerical prediction of convective occurrence, mode and location. *Wea. Forecasting*, **18**, 782-794.
- Fulton, R. A., J. P. Breidenbach, D. Seo, D. A. Miller, T. O'Bannon, 1998: The WSR-88D rainfall algorithm. *Wea. Forecasting*, **13**, 377-395.
- Gallus, W. A. and J. F. Bresch, 2006: Comparison of impacts of WRF dynamic core, physics package, and initial conditions on warm season rainfall forecasts, *Mon. Wea. Rev.*, **134**, 2632–2641.

- Gill, D., J. Michalakes, J. Dudhia, W. Skamarock, and S.G. Gopalakrishnan, 2004: Nesting in WRF 2.0. Papers presented at the 5th WRF/14th MM5 Users' Workshop NCAR. Boulder, CO. (<http://box.mmm.ucar.edu/mm5/workshop/ws04/Session6/Gill.Dave.pdf>)
- Janjic, Z. I., 1984: Non-linear advection schemes and energy cascade on semi-staggered grids. *Mon. Wea. Rev.*, **112**, 1234-1245.
- Janjic, Z. I., 1990: The step-mountain coordinate: physical package, *Mon. Wea. Rev.*, **118**, 1429–1443.
- Janjic, Z. I., 1996: The surface layer in the NCEP Eta Model. Eleventh Conference on Numerical Weather Prediction, Norfolk, VA, 19–23 August, Amer. Meteor. Soc., Boston, MA, 354–355.
- Janjic, Z. I., 2002: Nonsingular Implementation of the Mellor–Yamada Level 2.5 Scheme in the NCEP Meso model, NCEP Office Note, No. 437, 61 pp.
- Janjic, Z. I., 2003a: A nonhydrostatic model based on a new approach. *Meteor. Atmos. Phys.*, **82**, 271-285.
- Janjic, Z. I., 2003b: The NCEP WRF core and further development of its physical package. *5th Int. SRNWP Workshop on Non-Hydrostatic Modeling*, Bad Orb, Germany, 27-29 October.
- Janjic, Z. I., J. P. Gerrity Jr., and S. Nickovic, 2001: An alternative approach to nonhydrostatic modeling. *Mon. Wea. Rev.*, **129**, 1164-1178.
- Jankov, I., W.A., Gallus, M., Segal, B., Shaw, and S.E., Koch, 2005: The impact of different WRF model physical parameterizations and their interactions on warm season MCS rainfall. *Wea. Forecasting*, **20**, 1048-1060.
- Kumar, S. V., C. D. Peters-Lidard, Y. Tian, P. R. Houser, J. Geiger, S. Olden, L. Lighty, J. L. Eastman, B. Doty, P. Dirmeyer, J. Adams, K. Mitchell, E. F. Wood and J. Sheffield, 2006. Land Information System - An interoperable framework for high resolution land surface modeling. *Environmental Modeling & Software.* , **21**, 1402-1415.
- Lacis, A. A., and J. E. Hansen, 1974: A parameterization for the absorption of solar radiation in the earth's atmosphere. *J. Atmos. Sci.*, **31**, 118–133.
- Laird, N. F., D. A. R. Kristovich, R. M. Rauber, H. T. Ochs III, and L. J. Miller, 1995: The Cape Canaveral sea and river breezes: Kinematic structure and convective initiation. *Mon. Wea. Rev.*, **123**, 2942–2956.
- Lericos, T.P., Fuelberg, H.E., Watson, A.I., and Holle, R.L., 2002: Warm season lightning distributions over the Florida peninsula as related to synoptic patterns. *Wea. Forecasting*, **17**, 83-98.
- Lin, Y.-L., R. D. Farley, and H. D. Orville, 1983: Bulk parameterization of the snow field in a cloud model. *J. Climate Appl. Meteor.*, **22**, 1065–1092.
- Lin, Y. and K. E. Mitchell, 2005: The NCEP Stage II/IV hourly precipitation analyses: development and applications. Preprints, 19th Conf. on Hydrology, American Meteorological Society, San Diego, CA, 9-13 January 2005, Paper 1.2.
- Lohmann, D., K. E. Mitchell, P. R. Houser, E. F. Wood, J. C. Schaake, A. Robock, B. A. Cosgrove, J. Sheffield, Q. Duan, L. Luo, W. Higgins, R. T. Pinker, and J. D. Tarpley, 2004: Streamflow and water balance intercomparisons of four land surface models in the North American Land Data Assimilation System project, *J. Geophys. Res.*, **109**, D07S91, doi:10.1029/2003JD003517.
- Lynn, B.H., D.R. Stauffer, P. J. Wetzel, W. Tao, P. Alpert, N. Perlin, R.D. Baker, R. Munoz, A. Boone, and Y. Jia, 2001: Improved simulation of Florida summer convection using the PLACE land model and a 1.5-order turbulence parameterization coupled to the Penn State-NCAR Mesoscale Model. *Mon. Wea. Rev.*, **129**, 1441-1461.

- Manobianco, J. and Nutter, P.A. 1998: Evaluation of the 29 km Eta model. Part II: Subjective verification over Florida. *Wea. Forecasting*, **14**, 18-37.
- McGinley, J. A., 1995: Opportunities for high resolution data analysis, prediction, and product dissemination within the local weather office. *Preprints, 14th Conf. on Weather Analysis and Forecasting*, Dallas, TX, Amer. Meteor. Soc., 478-485.
- McGinley, J. A., and J. R. Smart, 2001: On providing a cloud-balanced initial condition for diabatic initialization. *14th Conf. on Numerical Weather Prediction*, Fort Lauderdale, FL, Amer. Meteor. Soc.
- McGinley, J. A., S. C. Albers, and P. A. Stamus, 1991: Validation of a composite convective index as defined by a real-time local analysis system. *Wea. Forecasting*, **6**, 337–356.
- McPherson, R. D., 1970: A numerical study of the effect of a coastal irregularity on the sea breeze. *J. Appl. Meteor.*, **9**, 767–777.
- Mitchell, K. E., D. Lohmann, P. R. Houser, E. F. Wood, J. C. Schaake, A. Robock, B. A. Cosgrove, J. Sheffield, Q. Duan, L. Luo, R. W. Higgins, R. T. Pinker, J. D. Tarpley, D. P. Lettenmaier, C. H. Marshall, J. K. Entin, M. Pan, W. Shi, V. Koren, J. Meng, B. H. Ramsay, and A. A. Bailey, 2004: The multi-institution North American Land Data Assimilation System (NLDAS): Utilizing multiple GCIP products and partners in a continental distributed hydrological modeling system. *J. Geophys. Res.*, **109**, D07S90, doi:10.1029/2003JD003823.
- Mlawer, E. J., S. J. Taubman, P. D. Brown, M. J. Iacono, and S. A. Clough, 1997: Radiative transfer for inhomogeneous atmosphere: RRTM, a validated correlated-k model for the longwave. *J. Geophys. Res.*, **102** (D14), 16663–16682.
- Olson, D. A., N. W. Junker, and B. Korty, 1995: Evaluation of 33 years of quantitative precipitation forecasting at NMC. *Wea. Forecasting*, **10**, 498–511.
- Peters-Lidard, C. D., S. Kumar, Y. Tian, J. L. Eastman, and P. Houser, 2004: Global urban-scale land-atmosphere modeling with the Land Information System. Symposium on Planning, Nowcasting, and Forecasting in the Urban Zone, 84th AMS Annual Meeting 11-15 January 2004 Seattle, WA, USA.
- Pielke, R. A., 1974: A three-dimensional numerical model of the sea breeze over south Florida. *Mon. Wea. Rev.*, **102**, 115–139.
- Pleim, J. E. and A. Xiu, 2003: Development of a Land Surface Model. Part II: Data assimilation. *J. Appl. Meteor.*, **42**, 1811-1822.
- Purdum, J. F. W., 1982: Subjective interpretation of geostationary satellite data for nowcasting. *Nowcasting*, K. Browning, Ed., Academic Press, 149–156.
- Reichle, R., 2005: Land Surface Assimilation. Retrieved from <http://gmao.gsfc.nasa.gov/research/landsurface/>.
- Roberts, N.M., 2005: An investigation of the ability of a storm-scale configuration of the Met Office NWP model to predict flood-producing rainfall. *Forecasting Research Tech. Rept. 455*, Met Office, 80 pp.
- Rodell, M., P. R. Houser, A. A. Berg, J. S. Famiglietti, 2005: Evaluation of 10 methods for initializing a Land Surface Model. *Journal of Hydrometeorology*, **6**, 146-155.
- Rozulmalski, R., 2006: WRF Environmental Modeling System User's Guide. NOAA/NWS SOO Science and Training Resource Coordinator Forecast Decision Training Branch, 89 pp. [Available from COMET/UCAR, P.O. Box 3000, Boulder, CO, 80307-3000].
- Schultz, P., and S. Albers, 2001: The use of three-dimensional analyses of cloud attributes for diabatic initialization of mesoscale models. *14th Conf. on Numerical Weather Prediction*, Fort Lauderdale, FL, Amer. Meteor. Soc.

- Schwarzkopf, M. D., and S. B. Fels, 1985: Improvements to the algorithm for computing CO₂ transmissivities and cooling rates. *J. Geophys. Res.*, **90**, 541-550.
- Schwarzkopf, M. D., and S. B. Fels, 1991: The simplified exchange method revisited: An accurate, rapid method for computations of infrared cooling rates and fluxes. *J. Geophys. Res.*, **96**, 9075-9096.
- Shaw, B. L., E. Thaler, and E. Szoke 2001: Operational evaluation of the LAPS–MM5 "hot start" local forecast model. *18th Conf. on Wea. Anal. And Fcst.*, Fort Lauderdale, FL, Amer. Meteor. Soc.
- Simpson, J., N. E. Westcott, R. J. Clerman, and R. A. Pielke, 1980: On cumulus mergers. *Arch. Meteor. Geophys. Bioklimatol. Ser. A.*, **29**, 1–40.
- Skamarock, W. C., J. B. Klemp, J. Dudhia, D. O. Gill, D. M. Barker, W. Wang, and J. G. Powers, 2005: A description of the Advanced Research WRF Version 2. NCAR Technical Note NCAR/TN-468+STR, 88 pp.
- Tao, W.-K., and J. Simpson, 1984: Cloud interactions and merging: Numerical simulations. *J. Atmos. Sci.*, **41**, 2901–2917.
- Xiu, A. and J. E. Pleim, 2001: Development of a Land Surface Model. Part I: Application in a mesoscale meteorological model. *J. Appl. Meteor.*, **40**, 192-209.
- Zhang, J., F. H. Carr, and K. Brewster, 1998: ADAS cloud analysis. Preprints, *12th Conf. on Numerical Weather Prediction*, Phoenix, AZ, Amer. Meteor. Soc., 185–188.

List of Acronyms

45 WS	45th Weather Squadron	NASA	National Aeronautics and Space Administration
ADAS	ARPS Data Analysis System	NCAR	National Center for Atmospheric Research
AMU	Applied Meteorology Unit	NCEP	National Centers for Environmental Prediction
ARPS	Advanced Regional Prediction System	NLDAS	North American Land Data Assimilation System
ARW	Advanced Research WRF	NMM	Non-hydrostatic Mesoscale Model
AWIPS	Advanced Weather Interactive Processing System	NOAA	National Oceanic and Atmospheric Administration
CCAFS	Cape Canaveral Air Force Station	NOAH	Community Noah Land Surface Model
CLM	Community Land Model	NWS	National Weather Service
EMS	Environmental Modeling System	RFC	River Forecast Center
FAWN	Florida Automated Weather Network	RUC	Rapid Update Cycle
FSS	Fractions Skill Score	SMG	Spaceflight Meteorology Group
GOES	Geostationary Operational Environmental Satellites	SOO	Science Operations Officer
GSD	Global Systems Division	SSEC	Space Science and Engineering Center
KSC	Kennedy Space Center	STRC	Science and Training Resource Center
LAPS	Local Analysis and Prediction System	VIC	Variable Infiltration Capacity
LDAS	Land Data Assimilation System	WRF	Weather Research and Forecasting
LIS	Land Information System	WSR-88D	Weather Surveillance Radar-1988 Doppler
LSM	Land Surface Model		
MLB	Melbourne, Florida		
NAM	North American Mesoscale		

NOTICE

Mention of a copyrighted, trademarked or proprietary product, service, or document does not constitute endorsement thereof by the author, ENSCO Inc., the AMU, the National Aeronautics and Space Administration, or the United States Government. Any such mention is solely for the purpose of fully informing the reader of the resources used to conduct the work reported herein.